

Efficient syntheses of pillar[6]arene-based hetero[4]rotaxanes using a cooperative capture strategy

Xisen Hou,^{‡a} Chenfeng Ke,^{‡a} Chuyang Cheng,^a Nan Song,^b Anthea K. Blackburn,^a Amy A. Sarjeant,^a
Yousry Y. Botros,^{c, d} Ying-Wei Yang,^{*, b} J. Fraser Stoddart^{*, a}

^a Department of Chemistry, Northwestern University, 2145 Sheridan Road, Evanston, IL 60208, USA.

^b State Key Laboratory of Supramolecular Structure and Materials, College of Chemistry, Jilin University, Changchun 130012, China.

^c University Research Office, Intel Corporation, Building RNB-6-61, 2200 Mission College Boulevard., Santa Clara, California 95054-1549, United States.

^d Joint Center of Excellence in Integrated Nano-Systems (JCIN), King Abdul-Aziz City for Science and Technology (KACST), P.O. Box 6086, Riyadh 11442, Kingdom of Saudi Arabia.

[‡] These authors contributed equally to this work.

Supplementary Information

CONTENTS

S1. Materials and General Methods

S2. Synthetic Procedures

S3. ¹H NMR Spectroscopy and Mass Spectroscopy

S4. Variant Temperature ¹H NMR Spectroscopy

S5. X-Ray Crystal Structure of the Hetero[4]rotaxane 2C4RexP₆·4PF₆

S6. Conformational Analysis

S1. Materials and General Methods

All reagents were purchased from commercial suppliers (Aldrich and Fisher) and used as received. The rod precursors¹ **2CV**·2PF₆ and **3CV**·2PF₆, pillar[6]arene² (P6), and stopper precursor³ (SP) were prepared as reported previously. Thin layer chromatography (TLC) was performed on silica gel 60 F254 (E. Merck). Column chromatography was carried out on silica gel 60F (Merck 9385, 0.040–0.063 mm). Nuclear magnetic resonance (NMR) spectra were recorded on Bruker Avance 500 or 600 spectrometers with working frequencies of 500 or 600 MHz for ¹H and 125 or 150 MHz for ¹³C nuclei, respectively. Chemical shifts are reported in ppm relative to the signals corresponding to the residual nondeuterated solvents (CD₃CN: δ = 1.94 ppm and (CD₃)₂CO: δ = 2.05 ppm). High-resolution electrospray ionization (HR-ESI) mass spectra were measured on an Agilent 6210 LC-TOF instrument with Agilent 1200 HPLC introduction.

S2. Synthetic Procedures

2CVex·2PF₆. 2-Azidoethyl-methanesulfonate⁴ (2 g, 8.30 mmol) and 4,4'-(1,4-phenylene)-bispyridine⁵ (450 mg, 1.94 mmol) were dissolved in anhydrous DMF (5 mL). The reaction mixture was stirred at 100 °C for 48 h before being cooled down to room temperature. The solvent was removed under reduced pressure and the residue was purified by column chromatography (SiO₂: gradient Me₂CO — 5% NH₄PF₆ in Me₂CO (m/v)). The fraction containing the product was collected, and the solvent was removed under reduced pressure. The resulting residue was washed with H₂O to remove excess of NH₄PF₆ and dried under high vacuum to afford **2CVex**·2PF₆ (940 mg, 73% yield) as a white powder. ¹H NMR (500 MHz, CD₃CN, 298 K): δ = 8.74 (d, *J* = 6.9 Hz,

4H), 8.37 (d, $J = 6.9$ Hz, 4H), 8.16 (s, 4H), 4.66 (t, $J = 5.5$ Hz, 4H), 3.98 (t, $J = 5.4$ Hz, 4H). ^{13}C NMR (125 MHz, CD_3CN , 298K): $\delta = 156.4, 146.0, 138.0, 130.4, 126.5, 60.7, 51.3$. HR-ESI-MS: calcd for $[M - \text{PF}_6]^+$ $m/z = 517.1448$, found $m/z = 517.1441$.

General procedure for the synthesis of hetero[4]rotaxanes. SP (91 μmol), the rod precursor (36 μmol) and P6 (50 μmol) were combined in MeCN (25 mL) and stirred at 25 °C (or 55 °C) for 18 h and monitored by TLC (SiO_2 , 2% NH_4PF_6 in Me_2CO (m/v)). As soon as the reactions were complete, the solvent was removed under reduced pressure and the residues were purified by column chromatography (SiO_2 : 0.2% NH_4PF_6 in Me_2CO and then 3% NH_4PF_6 in Me_2CO (m/v)). The fractions containing the products were collected and the solvents were removed under reduced pressure. The residue were washed with H_2O to remove excess of NH_4PF_6 and dried under high vacuum to afford the hetero[4]rotaxanes.

2C4R_{P6}•4PF₆. Following the general procedure, **2C4R_{P6}•4PF₆** was isolated as an orange powder (80 mg, 39% yield). ^1H NMR (500 MHz, CD_3CN , 298 K): $\delta = 9.43$ (d, $J = 6.3$ Hz, 4H), 7.94 (s, 4H), 7.32 (s, 12H), 6.95 (d, $J = 2.2$ Hz, 4H), 6.65 (s, 12H), 6.60 (s, 2H), 6.54 (t, $J = 2.3$ Hz, 2H), 6.15 – 6.11 (m, 4H), 5.87 (d, $J = 15.5$ Hz, 12H), 5.75 (d, $J = 15.3$ Hz, 12H), 5.36 (s, 24H), 5.31 – 5.25 (m, 4H), 4.51 – 4.41 (m, 8H), 4.39 – 4.32 (m, 4H), 4.27 (d, $J = 15.4$ Hz, 12H), 4.15 (d, $J = 15.3$ Hz, 12H), 3.87 (s, 15H), 3.58 (s, 12H). ^{13}C NMR (126 MHz, CD_3CN) δ 161.8, 157.3, 156.4, 149.3, 148.1, 147.4, 140.6, 134.1, 127.4, 125.6, 119.8, 109.1, 102.0, 70.9, 58.3, 56.1, 53.6, 52.4, 52.0, 48.6, 44.1, 30.4. HR-ESI-MS: calcd for $[M - 4\text{PF}_6]^{4+}$ $m/z = 858.8000$, found $m/z = 858.7996$, $[M - \text{H} - 4\text{PF}_6]^{3+}$ $m/z = 1144.7310$, found $m/z = 1144.7332$, $[M - 3\text{PF}_6]^{3+}$ $m/z = 1193.3883$, found $m/z = 1193.3897$, $[M - \text{H} - 3\text{PF}_6]^{2+}$ $m/z = 1789.5788$, found $m/z = 1789.5767$, $[M - 2\text{H} - 4\text{PF}_6]^{2+}$ $m/z = 1716.5928$, found $m/z = 1716.5923$, $[M - 2\text{PF}_6]^{2+}$ $m/z = 1862.5648$, found $m/z = 1862.5650$.

3C4R_{P6}·4PF₆. Following the general procedure, **3C4R_{P6}·4PF₆** was isolated as a pale orange powder (51 mg, 38% yield). ¹H NMR (500 MHz, CD₃CN, 298 K): δ = 8.54 (d, *J* = 6.3 Hz, 4H), 8.08 (s, 4H), 7.55 (s, 12H), 6.93 (d, *J* = 2.3 Hz, 4H), 6.67 (s, 12H), 6.54 (t, *J* = 2.2 Hz, 2H), 6.46 (s, 2H), 6.32 (d, *J* = 6.1 Hz, 4H), 5.84 (d, *J* = 15.3, 12H), 5.72 (d, *J* = 15.2 Hz, 12H), 5.33 (s, 24H), 4.72 (t, *J* = 8.2 Hz, 4H), 4.40 (m, 8H), 4.21 (d, *J* = 15.4 Hz, 12H), 4.11 (d, *J* = 15.3 Hz, 12H), 3.85 (s, 12H), 3.59 (s, 12H), 3.56 (d, *J* = 7.0 Hz, 4H), 2.62 – 2.51 (m, 4H). ¹³C NMR (126 MHz, CD₃CN, 298 K) δ = 161.9, 157.0, 156.4, 148.1, 147.7, 145.8, 140.1, 134.5, 127.1, 125.1, 120.0, 101.7, 70.8, 60.6, 56.1, 52.9, 52.2, 51.9, 47.1, 44.3, 32.5, 30.7, 28.6. HR-ESI-MS: calcd for [*M* – 4PF₆]⁴⁺ *m/z* = 865.5570, found *m/z* = 865.5579, [*M* – H – 4PF₆]³⁺ *m/z* = 1153.7403, found *m/z* = 1153.7425, [*M* – 3PF₆]³⁺ *m/z* = 1202.3976, found *m/z* = 1202.3988, [*M* – H – 3PF₆]²⁺ *m/z* = 1803.0928, found *m/z* = 1803.0958.

2C4R_{exp6}·4PF₆. Following the general procedure, **2C4R_{exp6}·4PF₆** was isolated as an orange powder (100 mg, 68% yield). ¹H NMR (500 MHz, CD₃CN, 298 K) δ = 9.72 (d, *J* = 6.4 Hz, 4H), 7.97 (d, *J* = 14.7 Hz, 4H), 7.76 (d, *J* = 6.3 Hz, 4H), 7.70 (s, 12H), 6.96 (d, *J* = 2.3 Hz, 4H), 6.79 (s, 12H), 6.62 (s, 2H), 6.54 (t, *J* = 2.2 Hz, 2H), 6.00 (s, 4H), 5.81 (d, *J* = 15.4 Hz, 12H), 5.74 (d, *J* = 15.3 Hz, 12H), 5.34 (s, 24H), 5.29 – 5.21 (m, 4H), 4.65 – 4.57 (m, 4H), 4.52 – 4.45 (m, 4H), 4.36 (t, *J* = 6.0 Hz, 4H), 4.23 (d, *J* = 15.4 Hz, 12H), 4.13 (d, *J* = 15.3 Hz, 12H), 3.87 (s, 12H), 3.60 (s, 12H). ¹³C NMR (125 MHz, CD₃CN, 298 K) δ = 161.8, 157.0, 156.4, 147.5, 146.1, 140.5, 135.8, 134.2, 128.1, 127.5, 125.8, 119.4, 109.0, 101.9, 70.8, 57.9, 56.1, 53.5, 52.3, 52.0, 49.1, 44.2, 29.8. HR-ESI-MS: calcd for [*M* – 4PF₆]⁴⁺ *m/z* = 877.5570, found *m/z* = 877.5562, [*M* – H – 4PF₆]³⁺ *m/z* = 1169.7403, found *m/z* = 1169.7397, [*M* – 3PF₆]³⁺ *m/z* = 1218.3976, found *m/z* = 1218.3962, [*M* – H – 3PF₆]²⁺ *m/z* = 1827.0928, found *m/z* = 1827.0864.

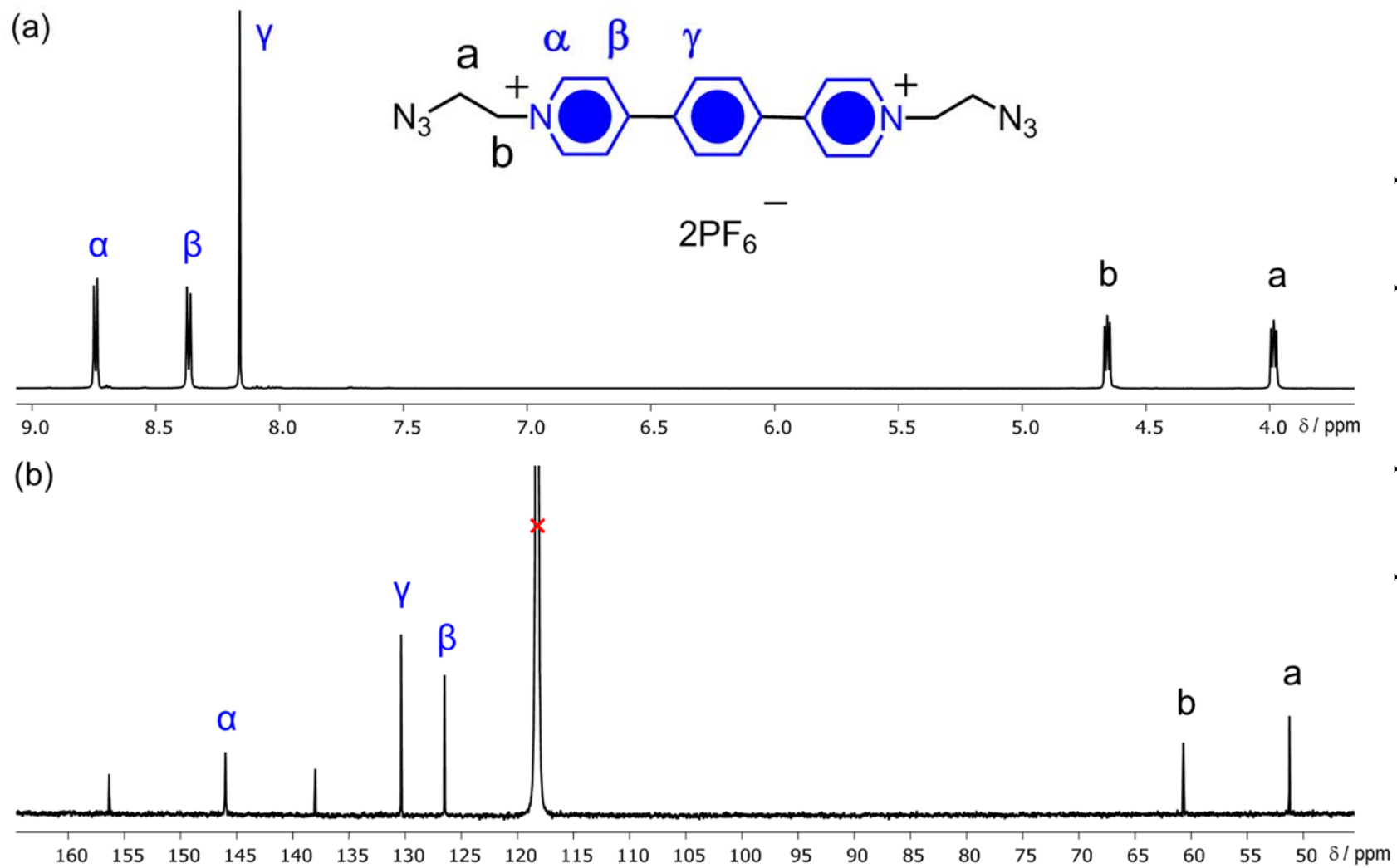


Figure S1. (a) ¹H NMR (500 MHz) and (b) ¹³C NMR (125 MHz) spectra of the rod precursor **2C4Rex**·2PF₆ in CD₃CN at 298 K.

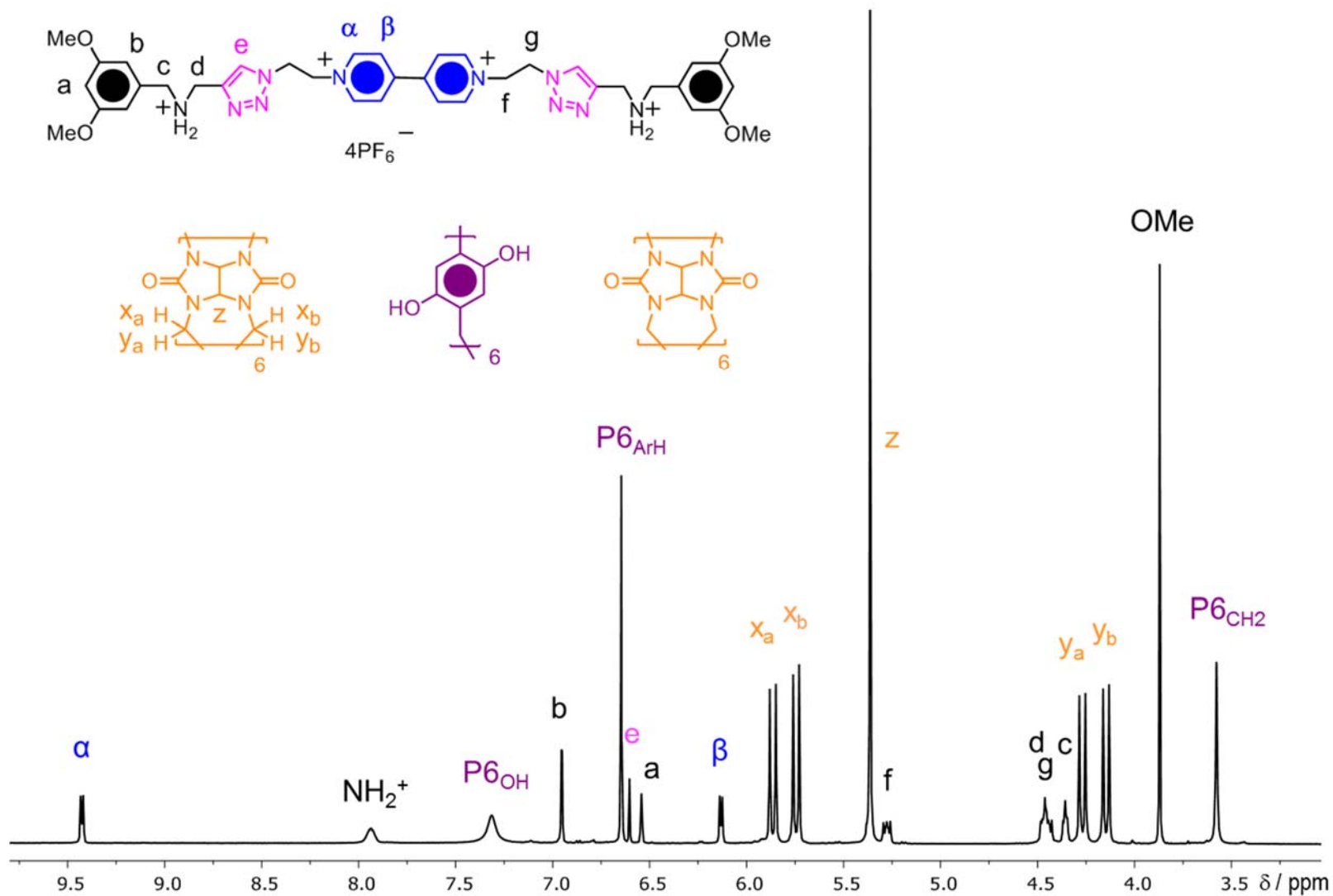


Figure S2. 1H NMR Spectrum (500 MHz, CD_3CN , 298 K) of $2C4R_{P6} \cdot 4PF_6$. Rather than illustrate the structural formula of the rotaxane $2C4R_{P6} \cdot 4PF_6$, its components with labeled protons are shown above.

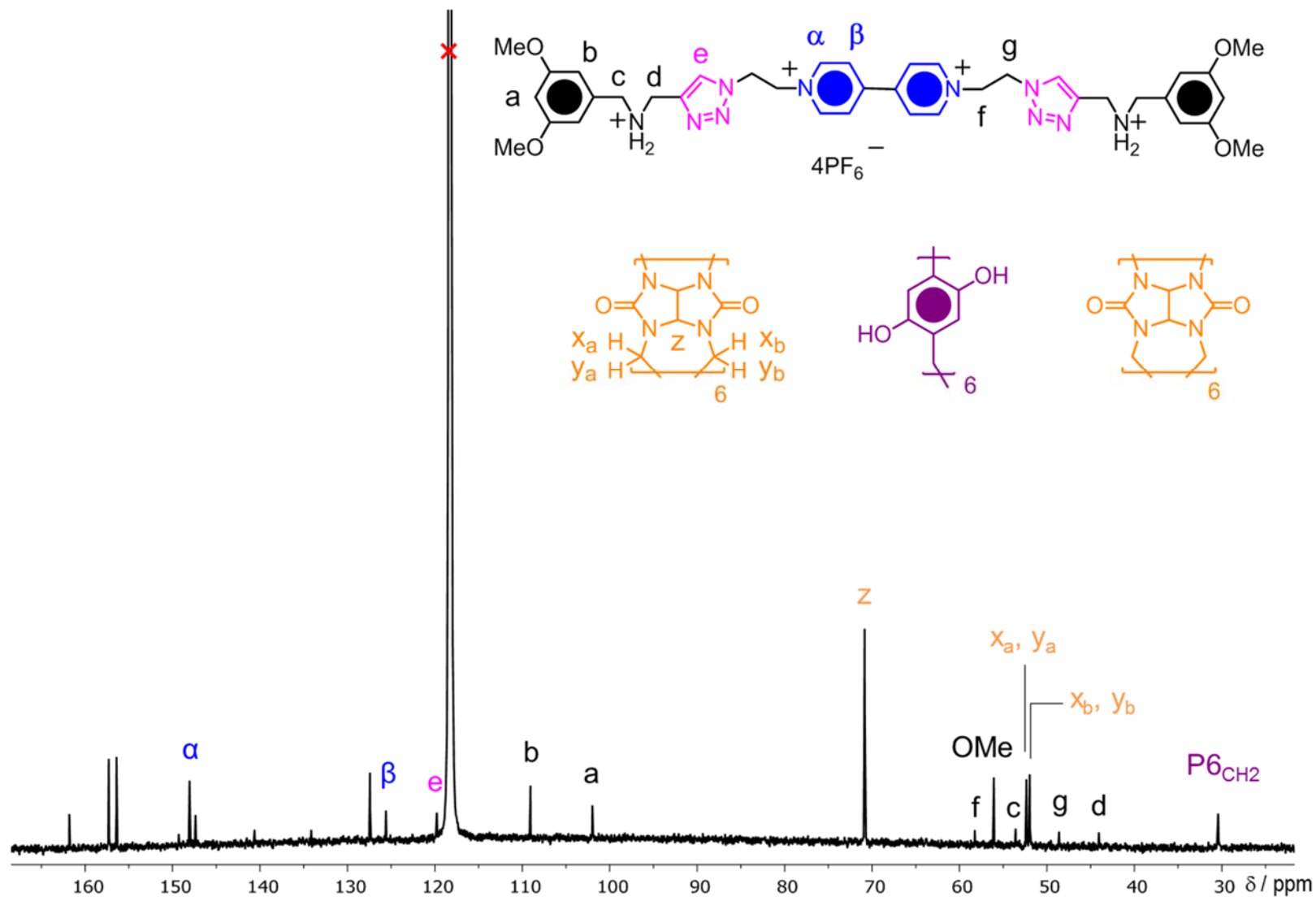


Figure S3. ^{13}C NMR Spectrum (125 MHz, CD_3CN , 298 K) of $2\text{C4R}_{\text{P6}} \cdot 4\text{PF}_6$. Rather than illustrate the structural formula of the rotaxane $2\text{C4R}_{\text{P6}} \cdot 4\text{PF}_6$, its components with labeled protons are shown above.

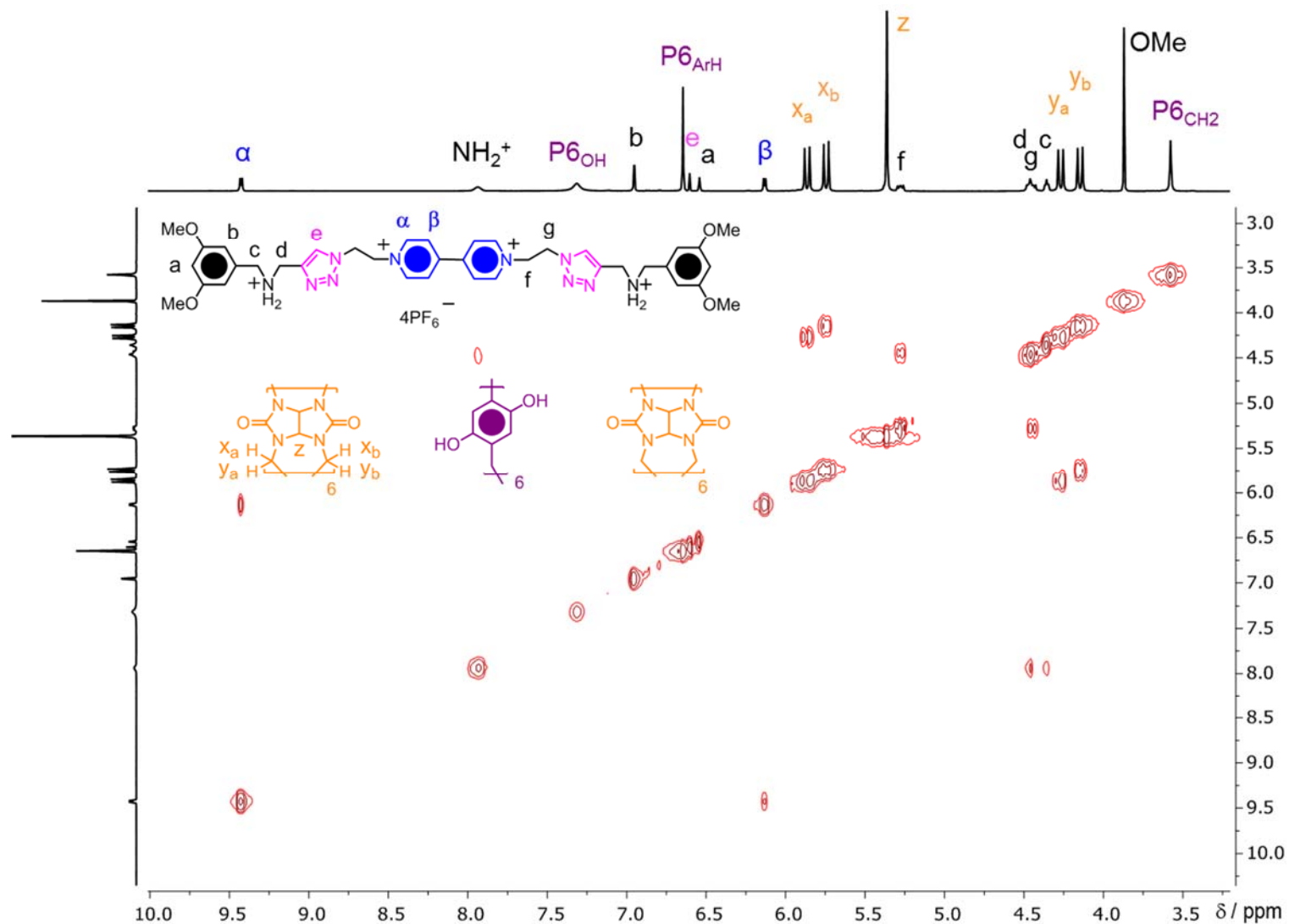


Figure S4. ^1H - ^1H COSY Spectrum (500 MHz, CD_3CN , 298 K) of $2\text{C}4\text{R}_{\text{P}6}\cdot 4\text{PF}_6$. Rather than illustrate the structural formula of the rotaxane $2\text{C}4\text{R}_{\text{P}6}\cdot 4\text{PF}_6$, its components with labeled protons are shown above.

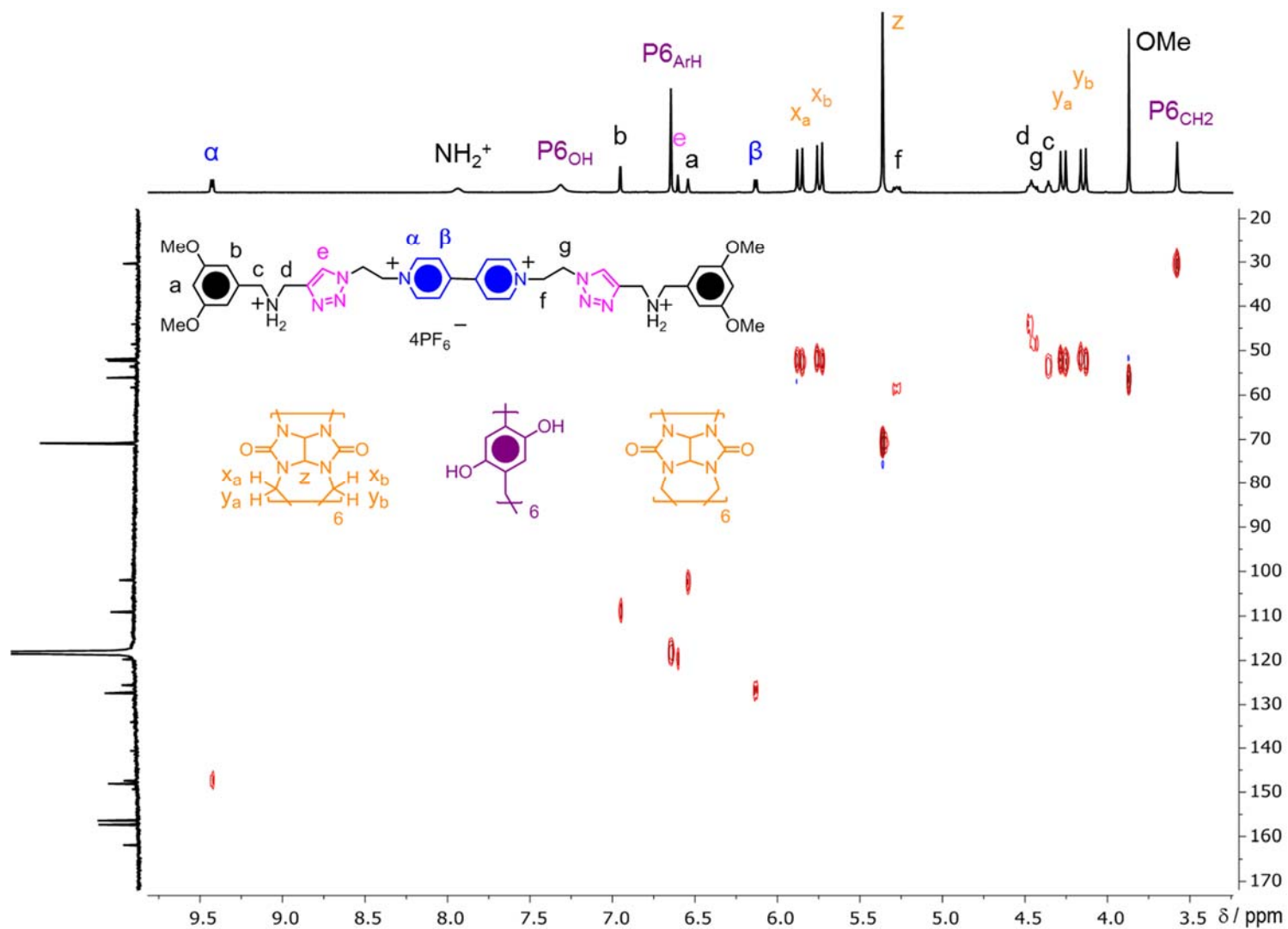


Figure S5. ^1H - ^{13}C HSQC Spectrum (500 MHz, CD_3CN , 298 K) of $2\text{C}4\text{R}_{\text{P}6}\cdot 4\text{PF}_6$. Rather than illustrate the structural formula of the rotaxane $2\text{C}4\text{R}_{\text{P}6}\cdot 4\text{PF}_6$, its components with labeled protons are shown above.

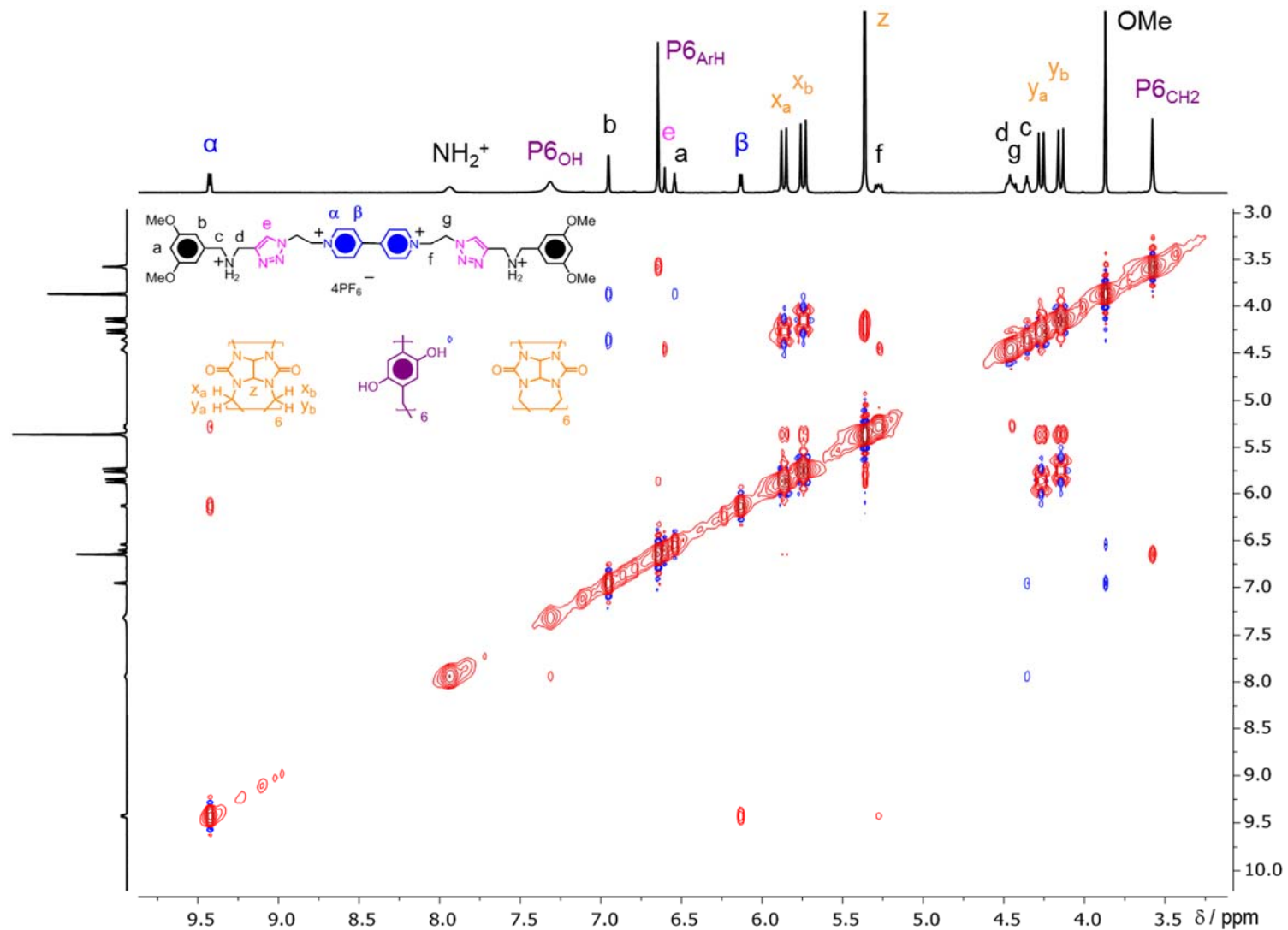


Figure S6. ^1H - ^1H NOESY Spectrum (500 MHz, CD_3CN , 298 K) of $2\text{C}4\text{R}_{\text{P}6}\cdot 4\text{PF}_6$. Rather than illustrate the structural formula of the rotaxane $2\text{C}4\text{R}_{\text{P}6}\cdot 4\text{PF}_6$, its components with labeled protons are shown above.

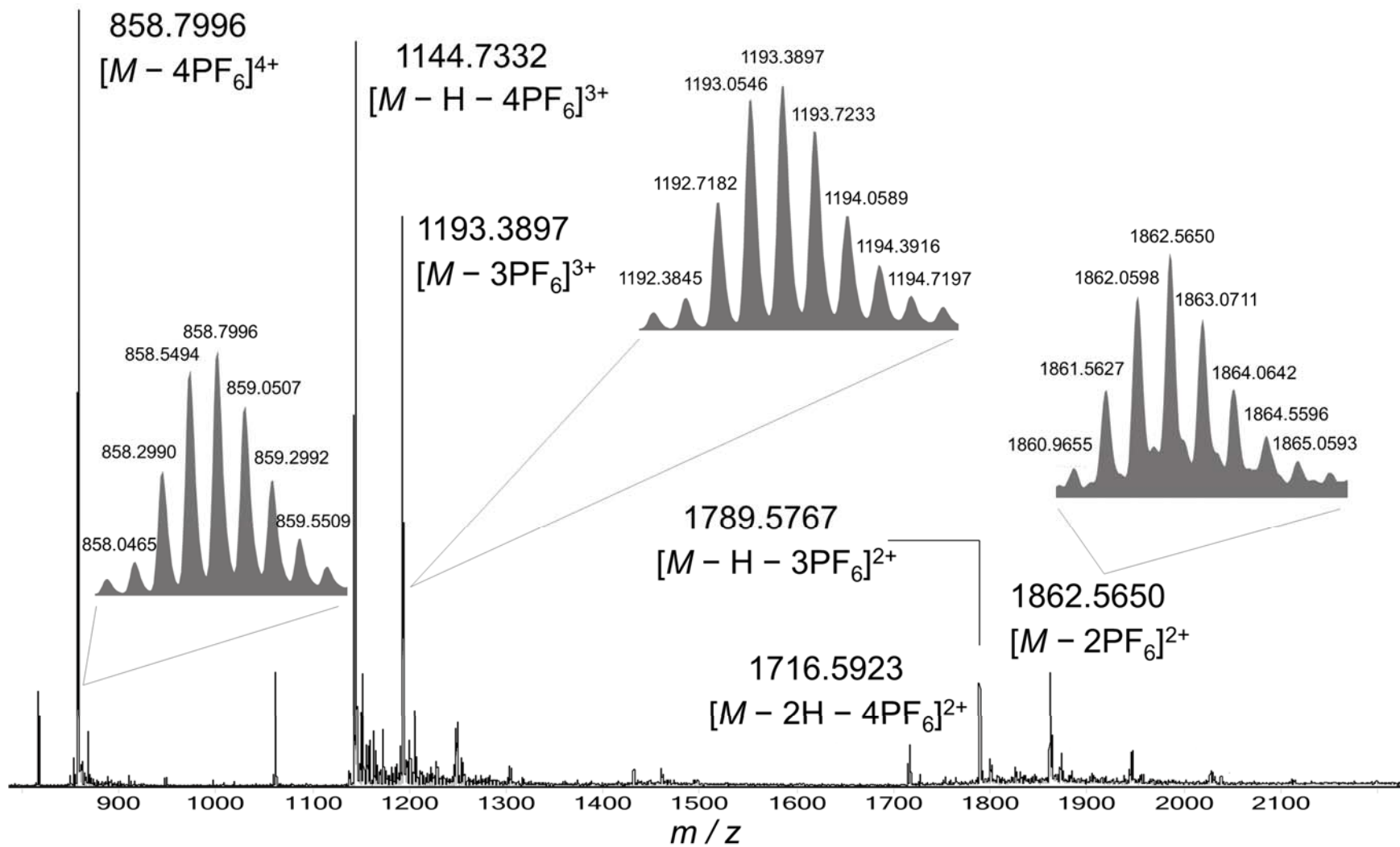


Figure S7. High resolution mass spectrum of $2C4R_{p6} \cdot 4PF_6$

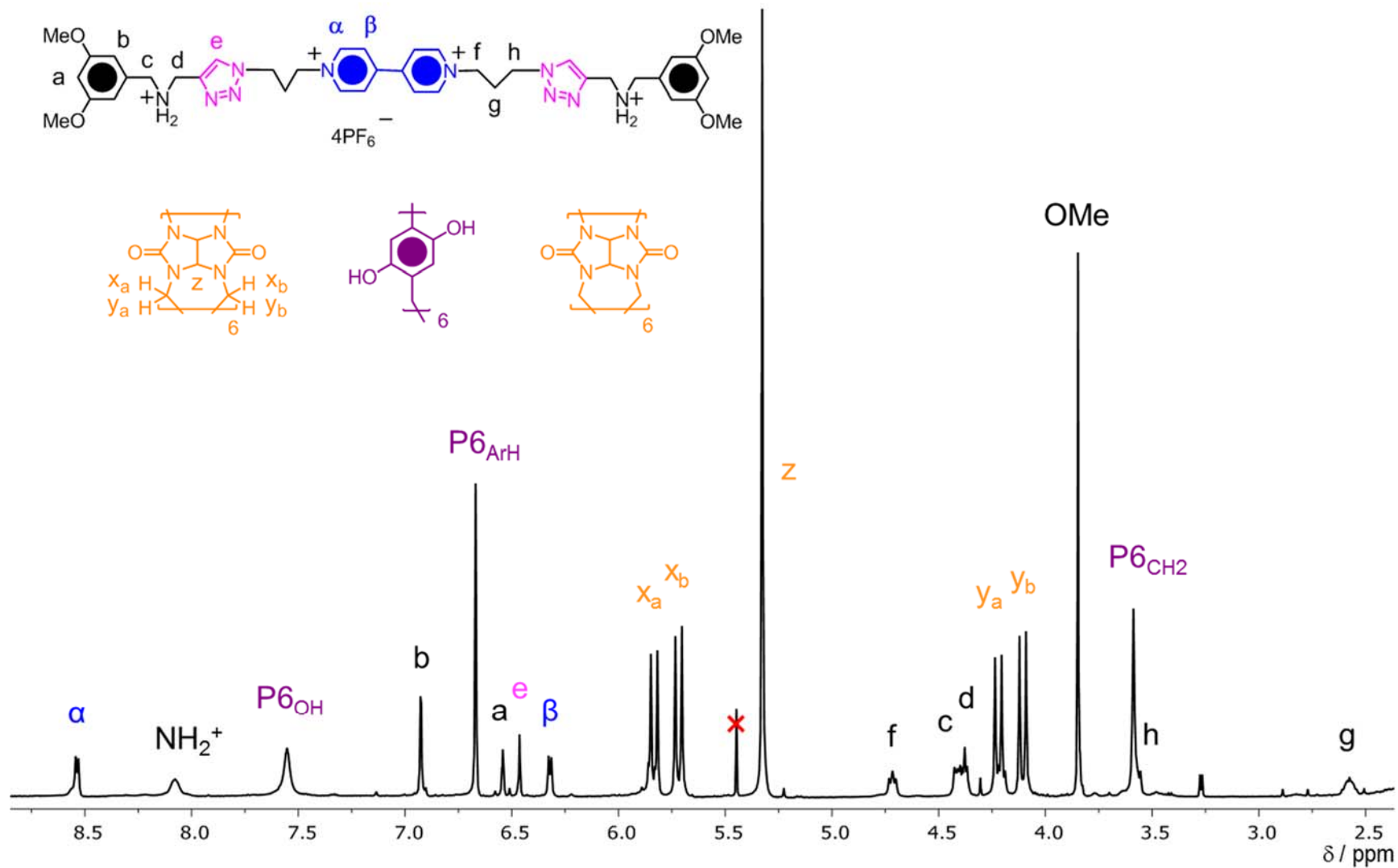


Figure S8. ¹H NMR Spectrum (500 MHz, CD₃CN, 298 K) of **3C4R_{P6}·4PF₆**. Rather than illustrate the structural formula of the rotaxane **3C4R_{P6}·4PF₆**, its components with labeled protons are shown above.

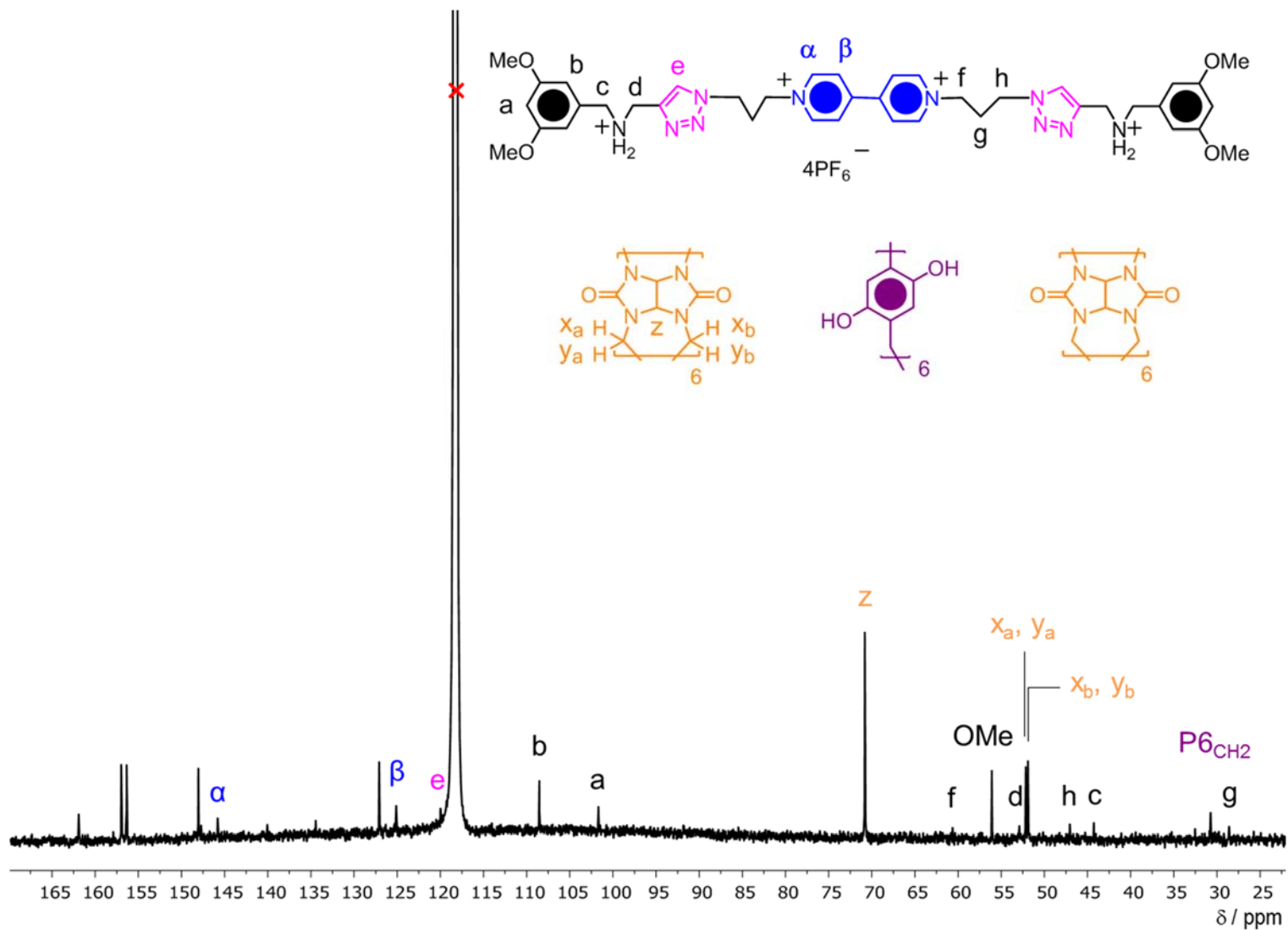


Figure S9. ^{13}C NMR Spectrum (125 MHz, CD_3CN , 298 K) of $3\text{C}4\text{R}_{\text{P}6} \cdot 4\text{PF}_6$. Rather than illustrate the structural formula of the rotaxane $3\text{C}4\text{R}_{\text{P}6} \cdot 4\text{PF}_6$, its components with labeled protons are shown above.

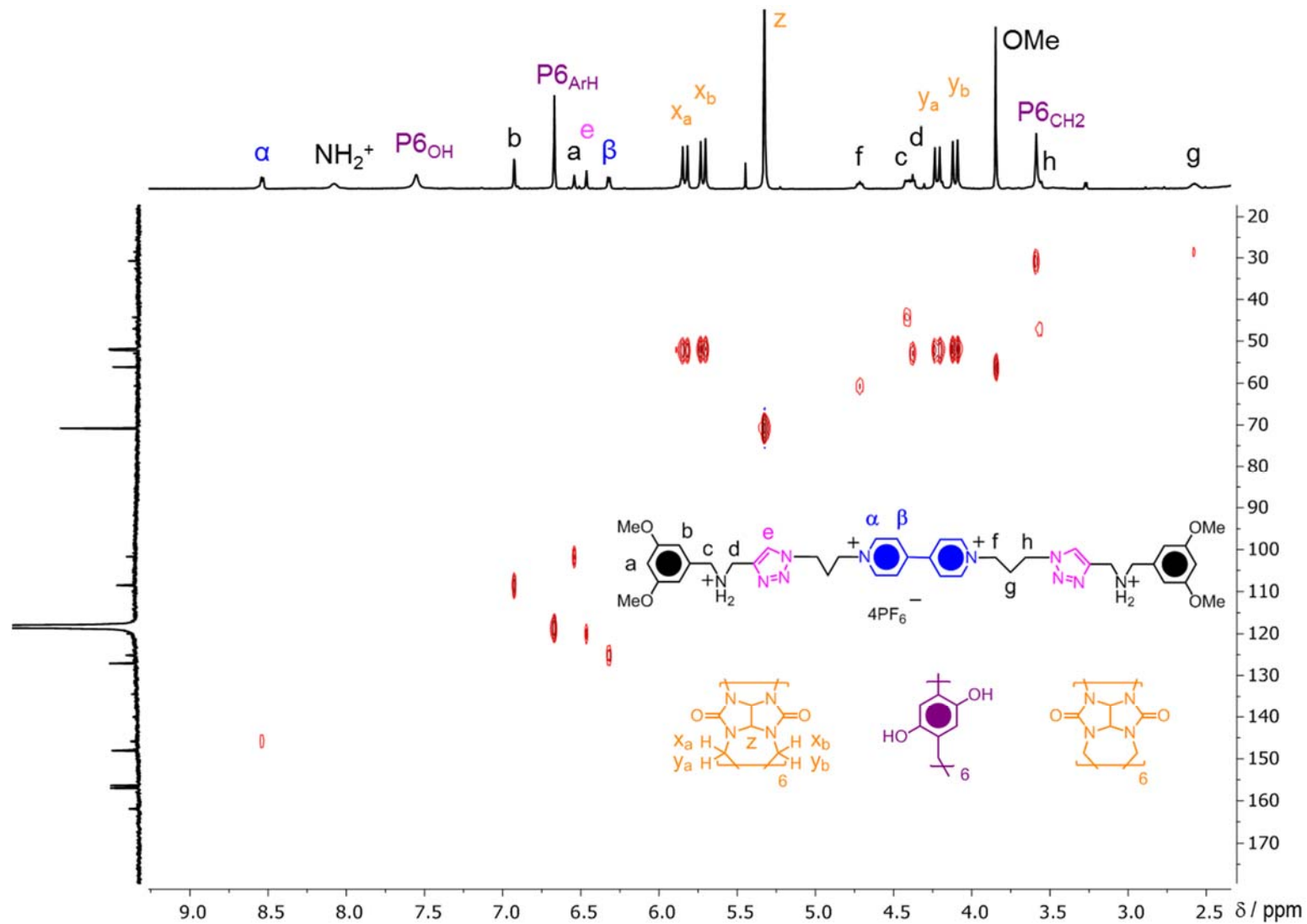


Figure S11. ^1H - ^{13}C HSQC Spectrum (500 MHz, CD_3CN , 298 K) of $3\text{C}4\text{R}_{\text{P}6}\cdot 4\text{PF}_6$. Rather than illustrate the structural formula of the rotaxane $3\text{C}4\text{R}_{\text{P}6}\cdot 4\text{PF}_6$, its components with labeled protons are shown above.

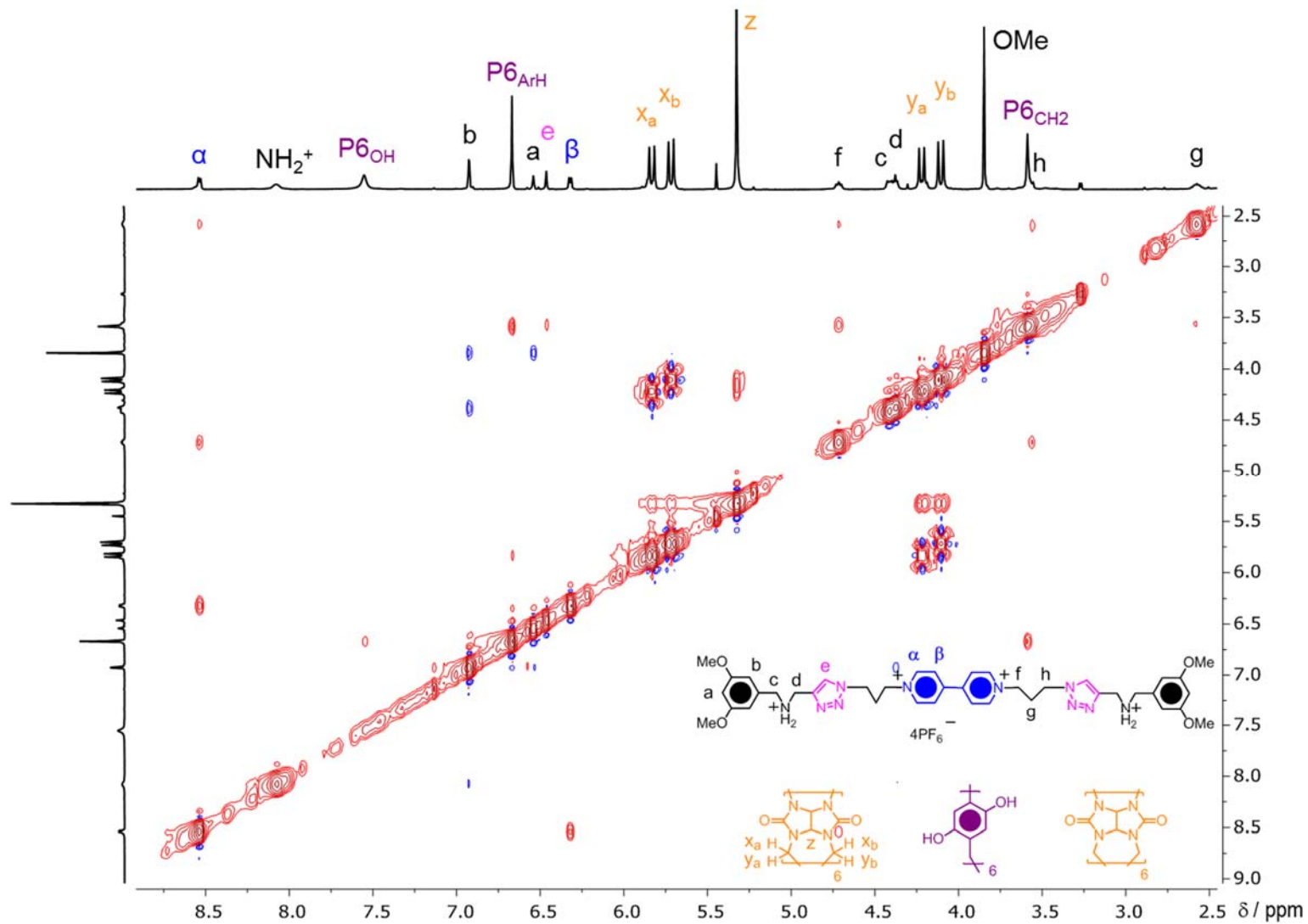


Figure S12. ^1H - ^1H NOESY Spectrum (500 MHz, CD_3CN , 298 K) of $3\text{C}4\text{R}_{\text{P}6}\cdot 4\text{PF}_6$. Rather than illustrate the structural formula of the rotaxane $3\text{C}4\text{R}_{\text{P}6}\cdot 4\text{PF}_6$, its components with labeled protons are shown above.

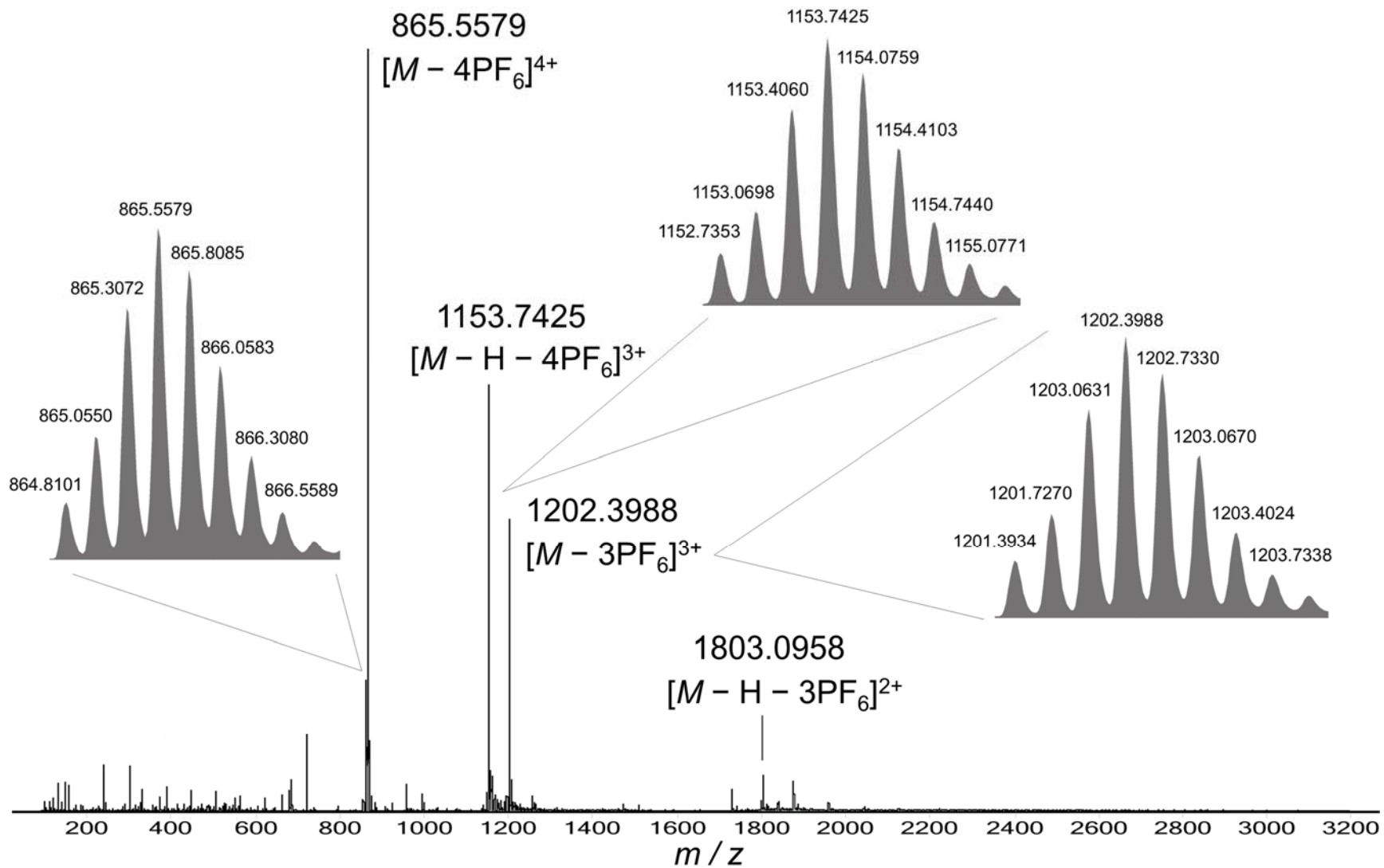


Figure S13. High resolution mass spectrum of $3C4R_{p6} \cdot 4PF_6$

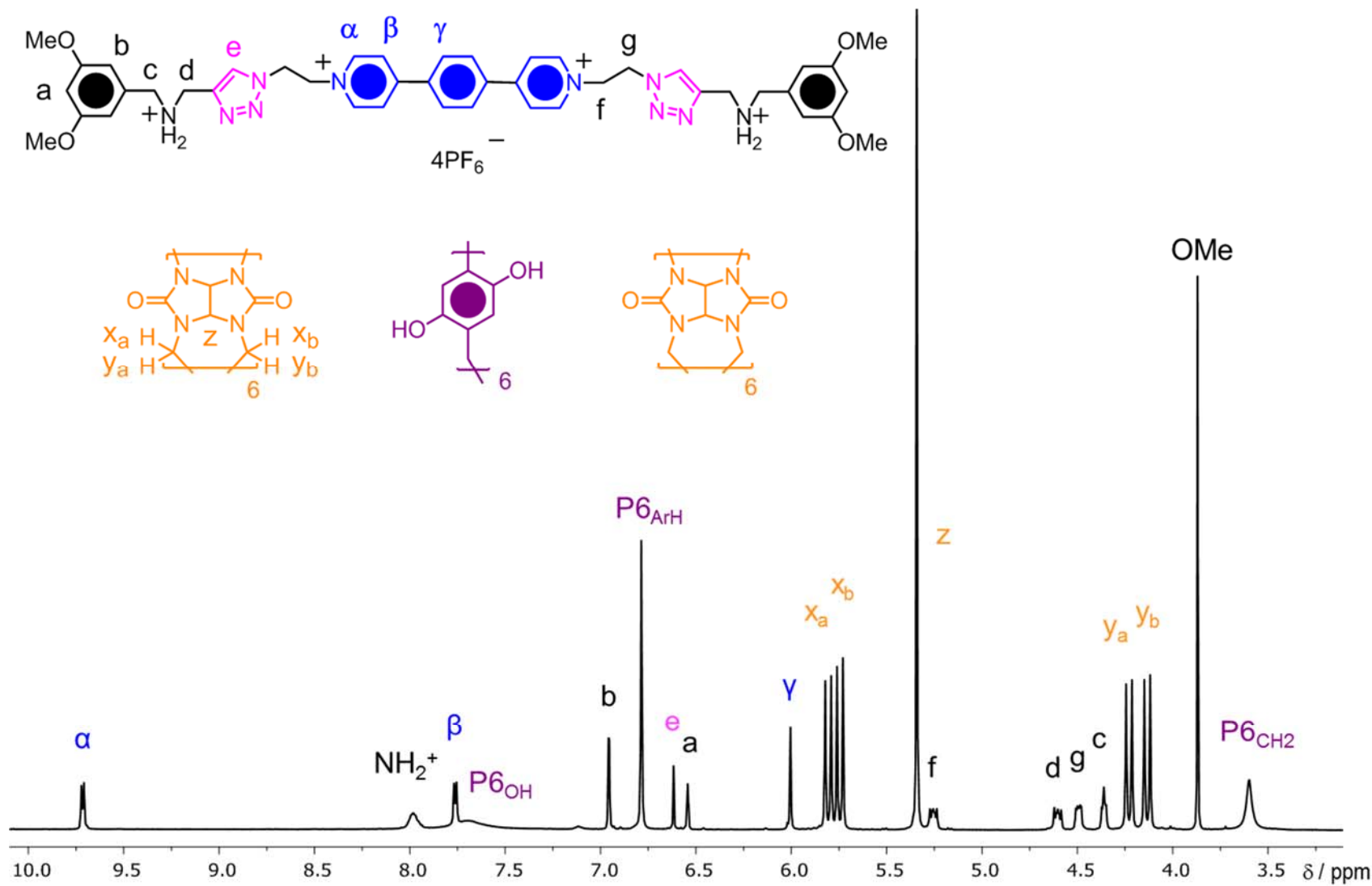


Figure S14. ^1H NMR Spectrum (500 MHz, CD_3CN , 298 K) of $2\text{C4RexP}_6 \cdot 4\text{PF}_6$. Rather than illustrate the structural formula of the rotaxane $2\text{C4RexP}_6 \cdot 4\text{PF}_6$, its components with labeled protons are shown above.

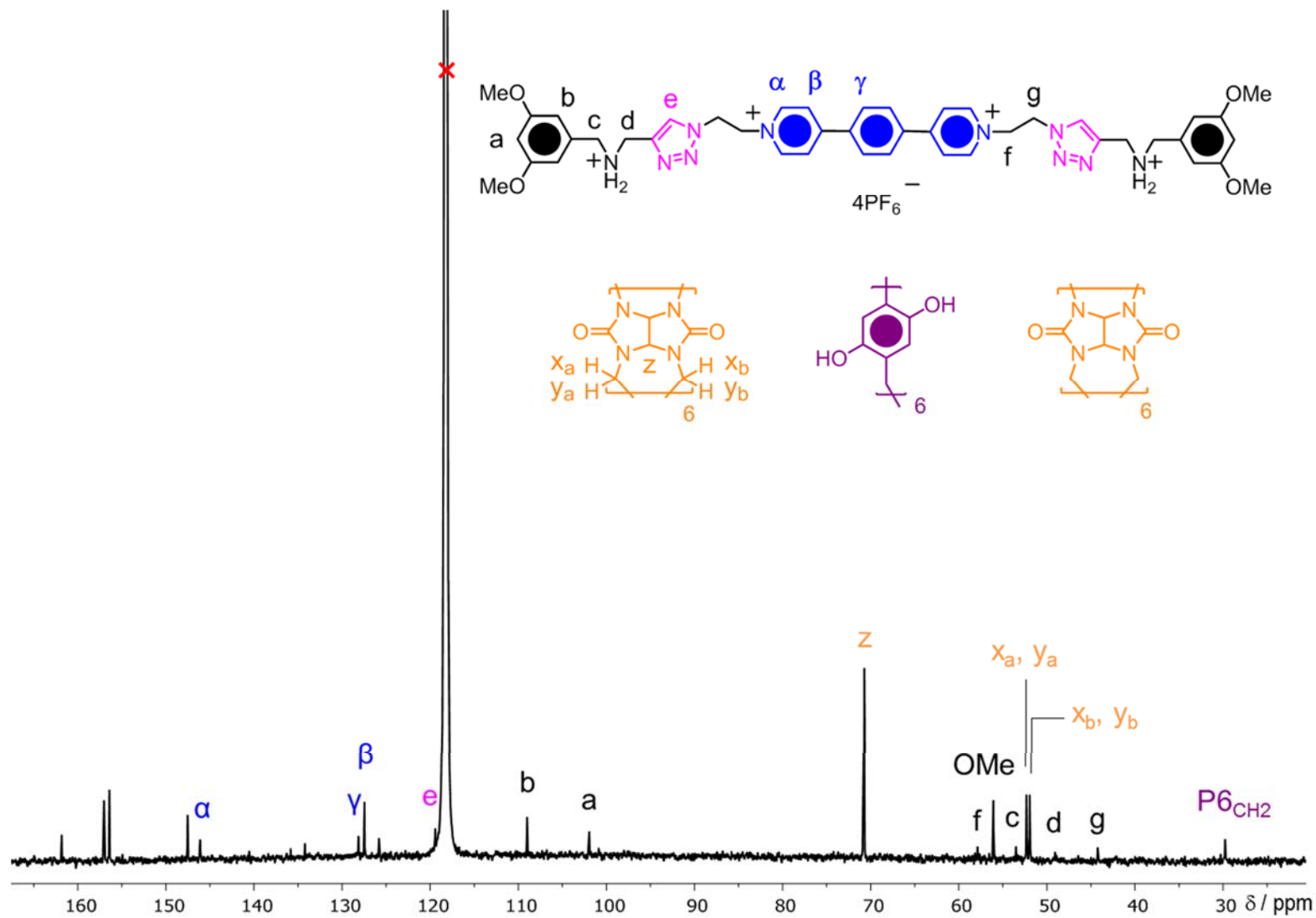


Figure S15. ¹³C NMR Spectrum (125 MHz, CD₃CN, 298 K) of **2C4RexP6**·4PF₆. Rather than illustrate the structural formula of the rotaxane **2C4RexP6**·4PF₆, its components with labeled protons are shown above.

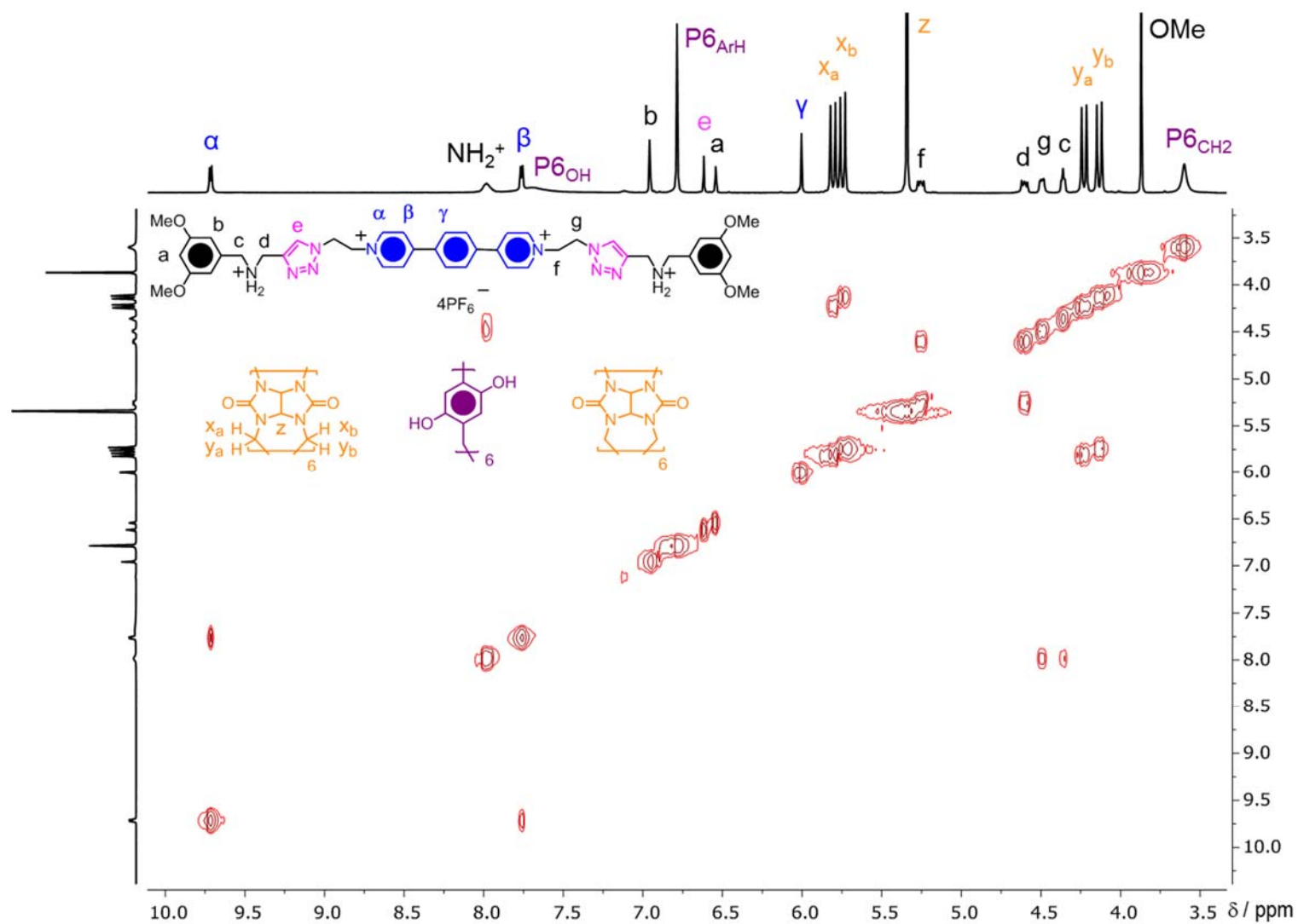


Figure S16. ^1H - ^1H COSY Spectrum (500 MHz, CD_3CN , 298 K) of $2\text{C4RexP}_6 \cdot 4\text{PF}_6$. Rather than illustrate the structural formula of the rotaxane $2\text{C4RexP}_6 \cdot 4\text{PF}_6$, its components with labeled protons are shown above.

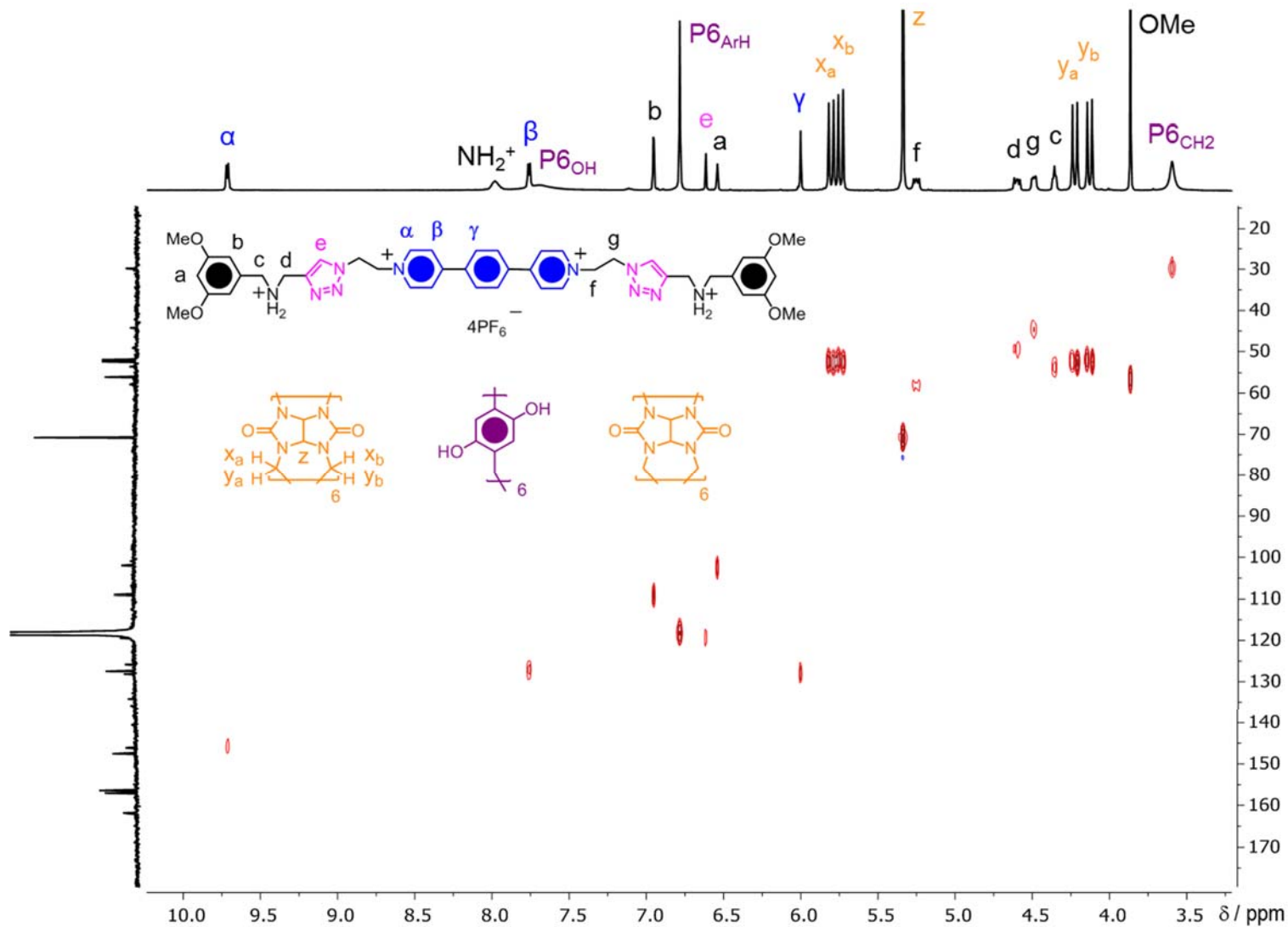


Figure S17. ^1H - ^{13}C HSQC Spectrum (500 MHz, CD_3CN , 298 K) of $2\text{C}4\text{RexP}6 \cdot 4\text{PF}_6$. Rather than illustrate the structural formula of the rotaxane $2\text{C}4\text{RexP}6 \cdot 4\text{PF}_6$, its components with labeled protons are shown above.

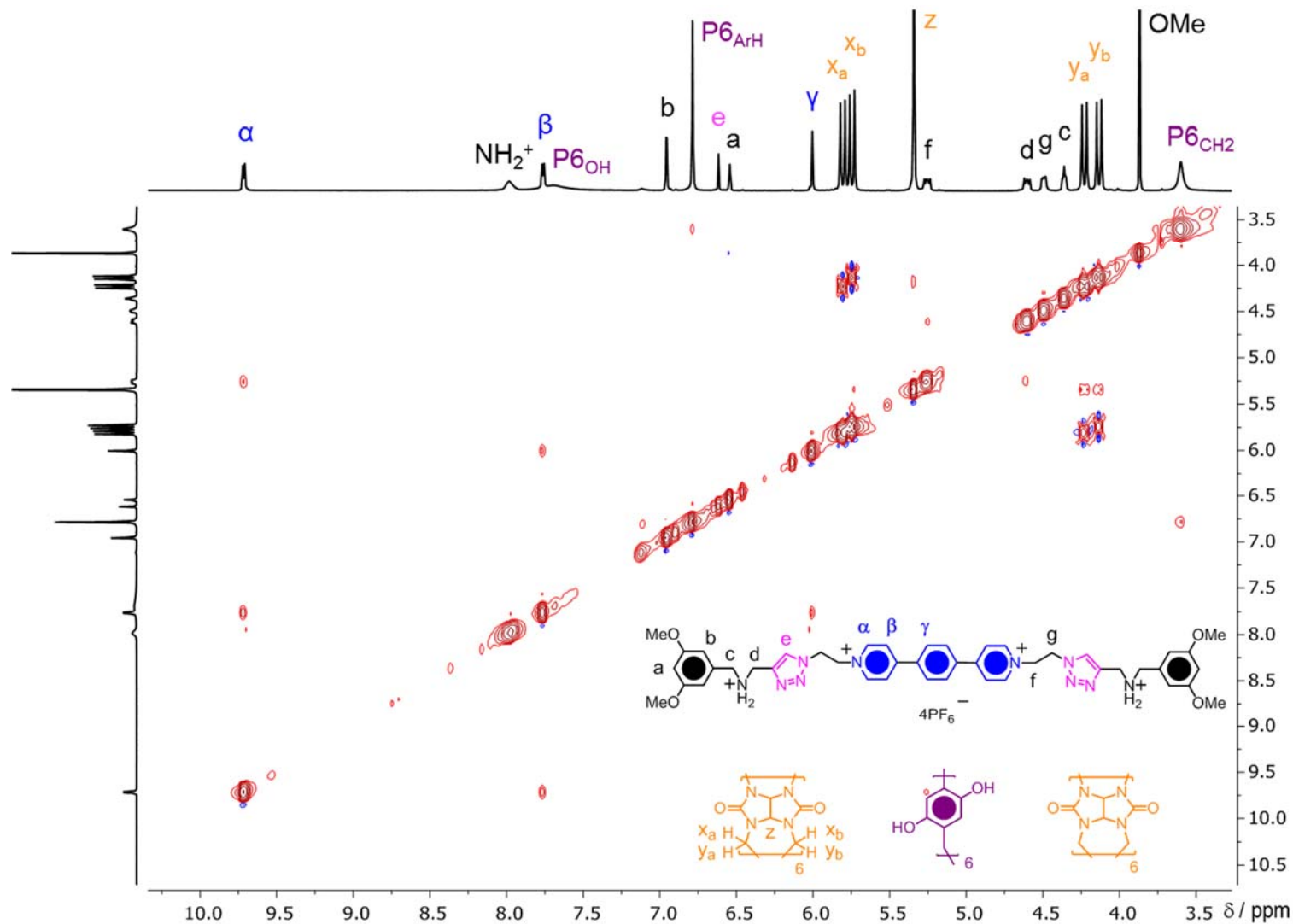


Figure S18. ^1H - ^1H NOESY Spectrum (500 MHz, CD_3CN , 298 K) of $2\text{C4RexP6} \cdot 4\text{PF}_6$. Rather than illustrate the structural formula of the rotaxane $2\text{C4RexP6} \cdot 4\text{PF}_6$, its components with labeled protons are shown above.

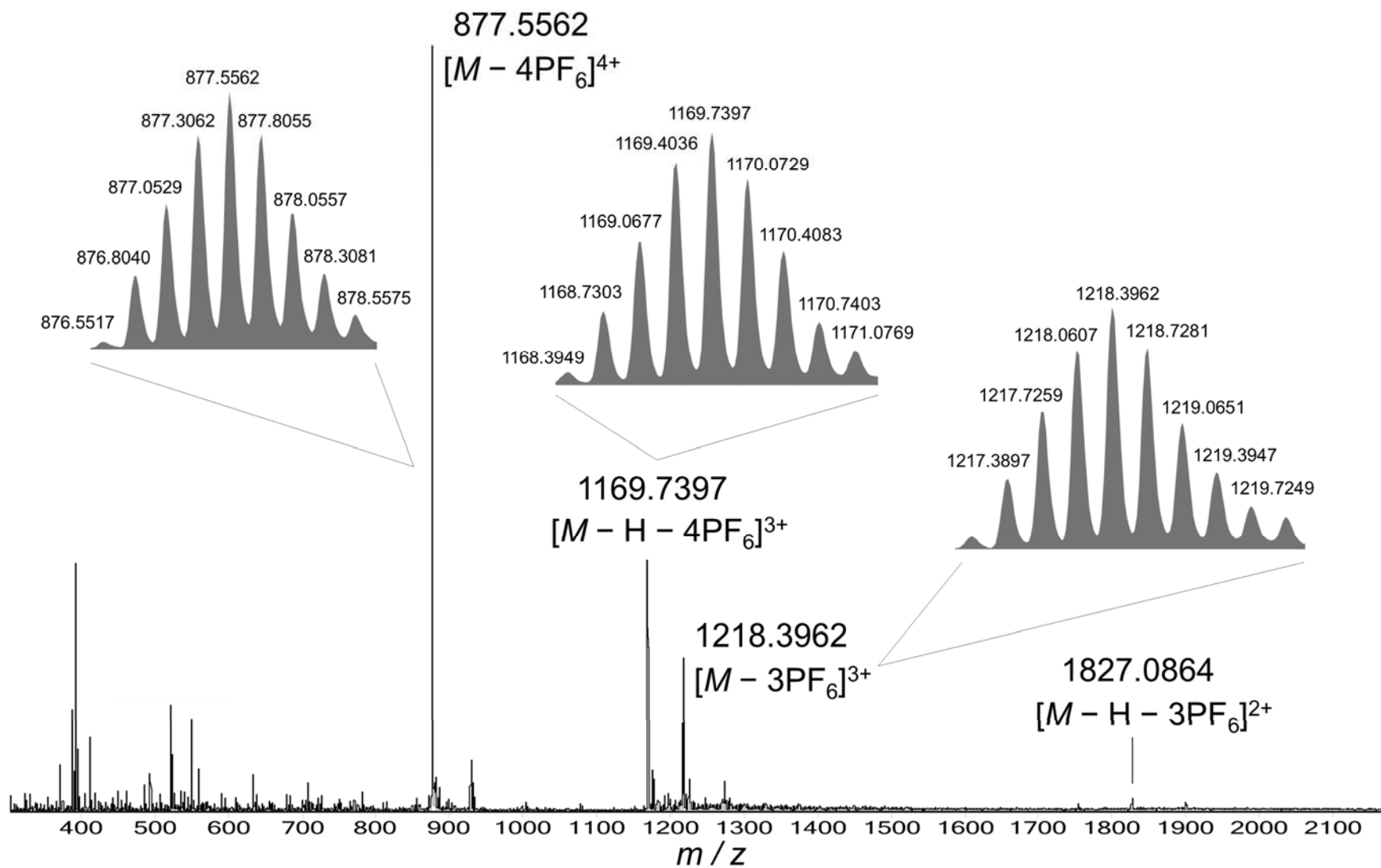


Figure S19. High resolution mass spectrum of $2C4R_{exp6} \cdot 4PF_6$.

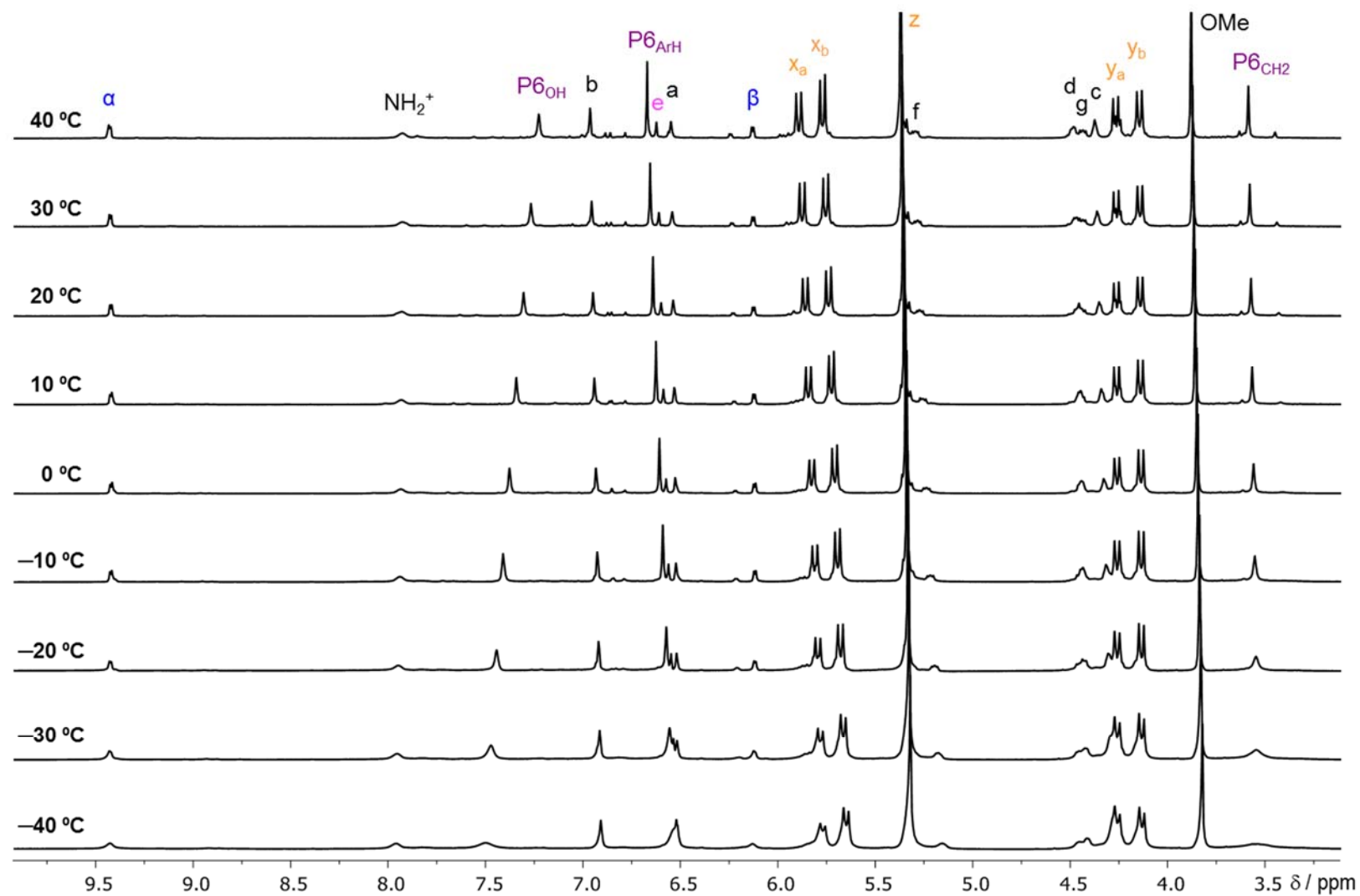


Figure S20. Temperature dependent ^1H NMR spectra (600 MHz, CD_3CN) of $2\text{C4RPF}_6 \cdot 4\text{PF}_6$.

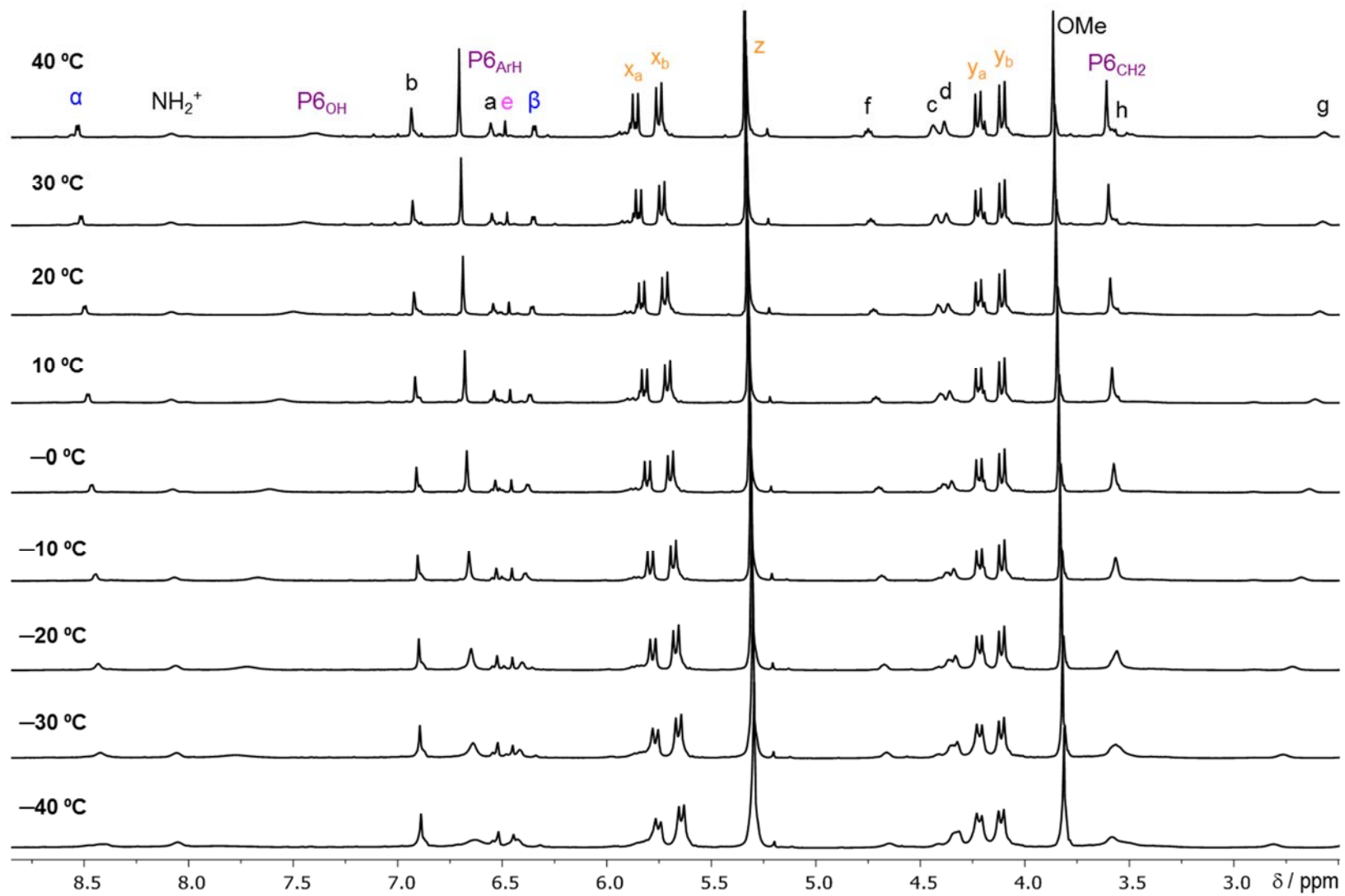


Figure S21. Temperature dependent ^1H NMR spectra (600 MHz, CD_3CN) of $3\text{C4R}_{\text{P6}} \cdot 4\text{PF}_6$.

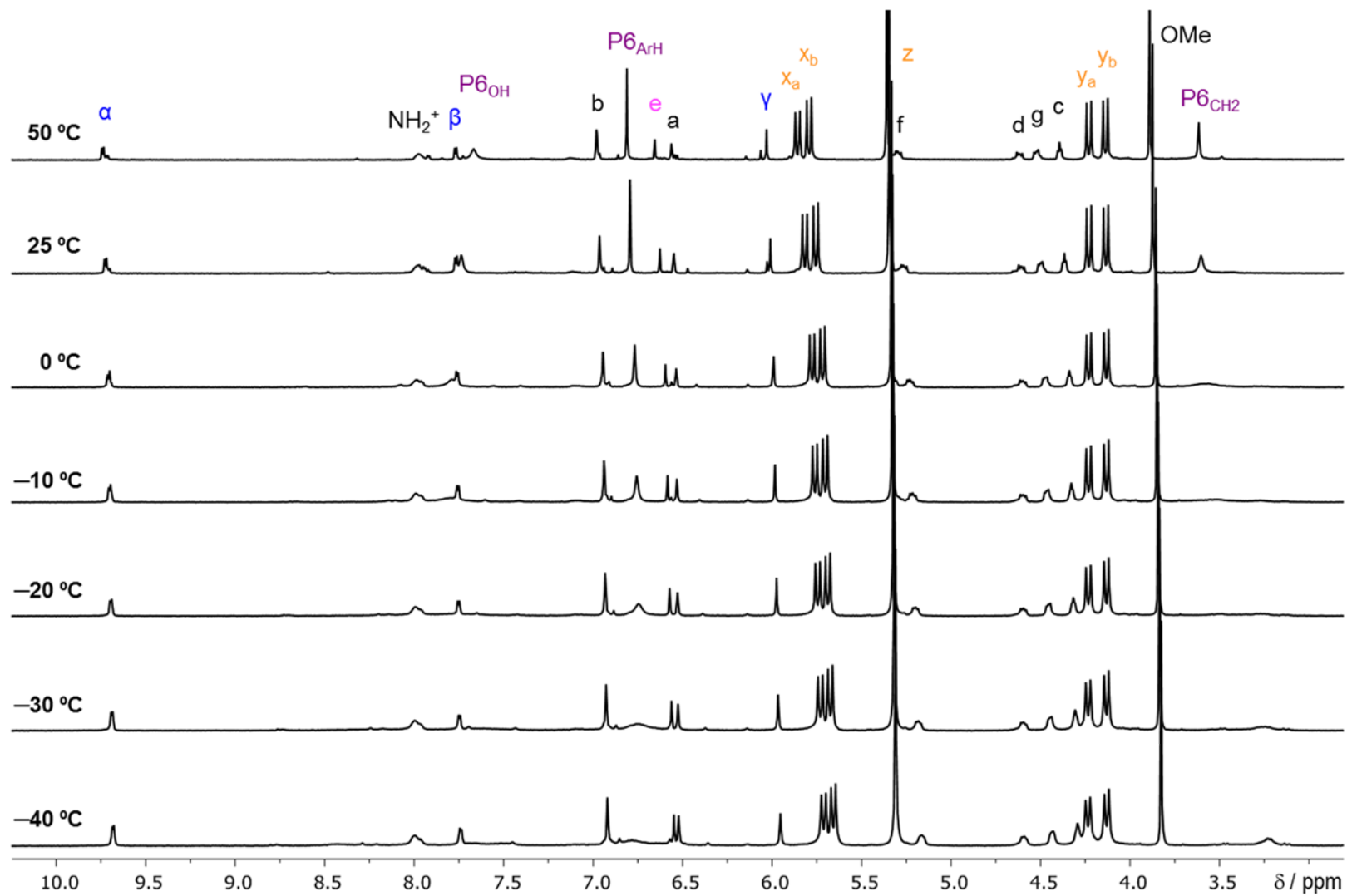


Figure S22. Temperature dependent ^1H NMR spectra (600 MHz, CD_3CN) of $2\text{C4RexP6}\cdot 4\text{PF}_6$.

S5. X-Ray Crystal Structure of the Hetero[4]rotaxane **2C4Rex_{P6}**·4PF₆

Crystals were grown by slow vapor diffusion of *i*-Pr₂O into a MeCN solution of **2C4Rex_{P6}**·4PF₆.

Crystal data for **2C4Rex_{P6}**·4PF₆:

2(C₃₆H₃₆N₂₄O₁₂)·(C₄₄H₅₂N₁₀O₄)·(C₄₂H₃₆O₁₂)·5(CH₃NO₂)·4(PF₆); colorless plate, 0.596 × 0.182 × 0.054 mm³, triclinic, space group $P\bar{1}$; $a = 16.0511(5)$, $b = 25.4637(9)$, $c = 30.2922(10)$ Å; $\alpha = 91.6273(18)$, $\beta = 94.4694(18)$, $\gamma = 90.902(2)$; $V = 12336.4(7)$ Å³; $Z = 2$; $\rho_{\text{calcd}} = 1.184$ g cm⁻³; $2\theta_{\text{max}} = 54.13^\circ$; $T = 100(2)$ K; 41702 reflections collected, 29486 independent, 2765 parameters; $\mu = 1.804$ mm⁻¹; $R_1 = 0.1284$ [$I > 2.0\sigma(I)$], $wR_2 = 0.3725$ (all data); CCDC deposition number 983503. The central phenyl ring of the rotaxane dumbbell exhibited a large amount of disorder, which modeling (AFIX 66) did not improve significantly. The terminal triazole rings of the dumbbell also showed disorder and were modeled using distance restraints and a group displacement parameter. An enhanced rigid-bond restraint (RIGU) was used globally. The solvent masking procedure as implemented in Olex2 was used to remove the electronic contribution of solvent molecule from the refinement. Only the atoms used in the refinement model are reported in the formula here. Total solvent accessible volume / cell = 4014.2 Å³ [32.5 %] Total electron / cell = 1130.1.

S6. Molecular Mechanics Simulation

The hetero[5]rotaxane **2C5Rex_{P6}** was subjected to an energy minimization employing the PRCG method for a maximum of 2000 iterations and a convergence threshold of 0.05 in Macromodel 9.1 using the OPLS-2005 force field and an implicit water solvation model.

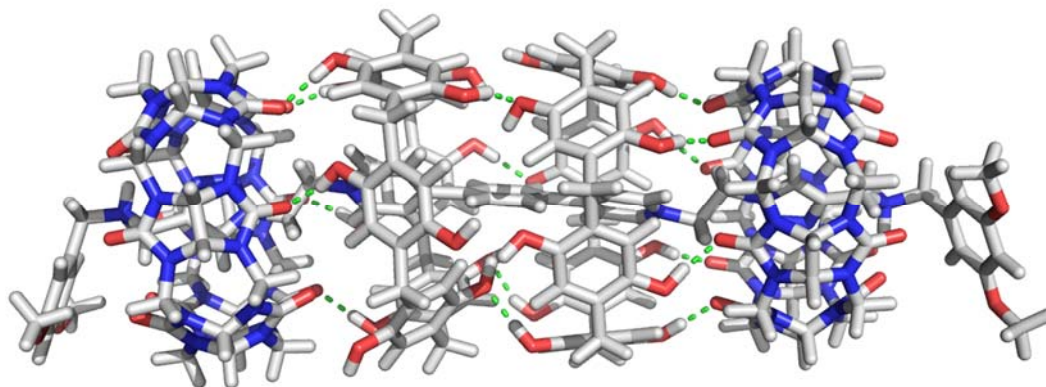


Figure S23. Energy-minimized structure of hetero[5]rotaxane **2C5Rexp₆**.

S7. Conformational Analysis

All conformational analyses were performed in MacroModel 9.1 using the OPLS-2005 force field and an implicit water solvation model. The structure of each conformational isomer of the hetero[4]rotaxanes **2C4R_{P6}·4PF₆**, **3C4R_{P6}·4PF₆** and **2C4Rexp₆·4PF₆** was constructed based on the X-ray crystal conformational isomer F of **2C4Rexp₆·4PF₆** and energy-minimized with the PRCG method for a maximum of 2000 iterations and a convergence threshold of 0.05. A conformational search was performed to determine the lowest energy conformation of each conformational isomer of the three hetero[4]rotaxanes. Each conformational search was performed using the large-scale low-mode sampling method. The maximum number of structures generated was 5000, with a maximum of 2000 unique structures to be saved per rotatable bond. Higher energy structures were removed using an energy cutoff of 5.02 kcal/mol. Each resulting structure was subjected to further minimization using the PRCG method with a maximum of 2000 iterations and a convergence threshold of 0.05. The lowest energy structure of each conformational isomer of the hetero[4]rotaxane **2C4R_{P6}·4PF₆**, **3C4R_{P6}·4PF₆** and **2C4Rexp₆·4PF₆** was determined and shown in Fig. S23-S25, respectively.

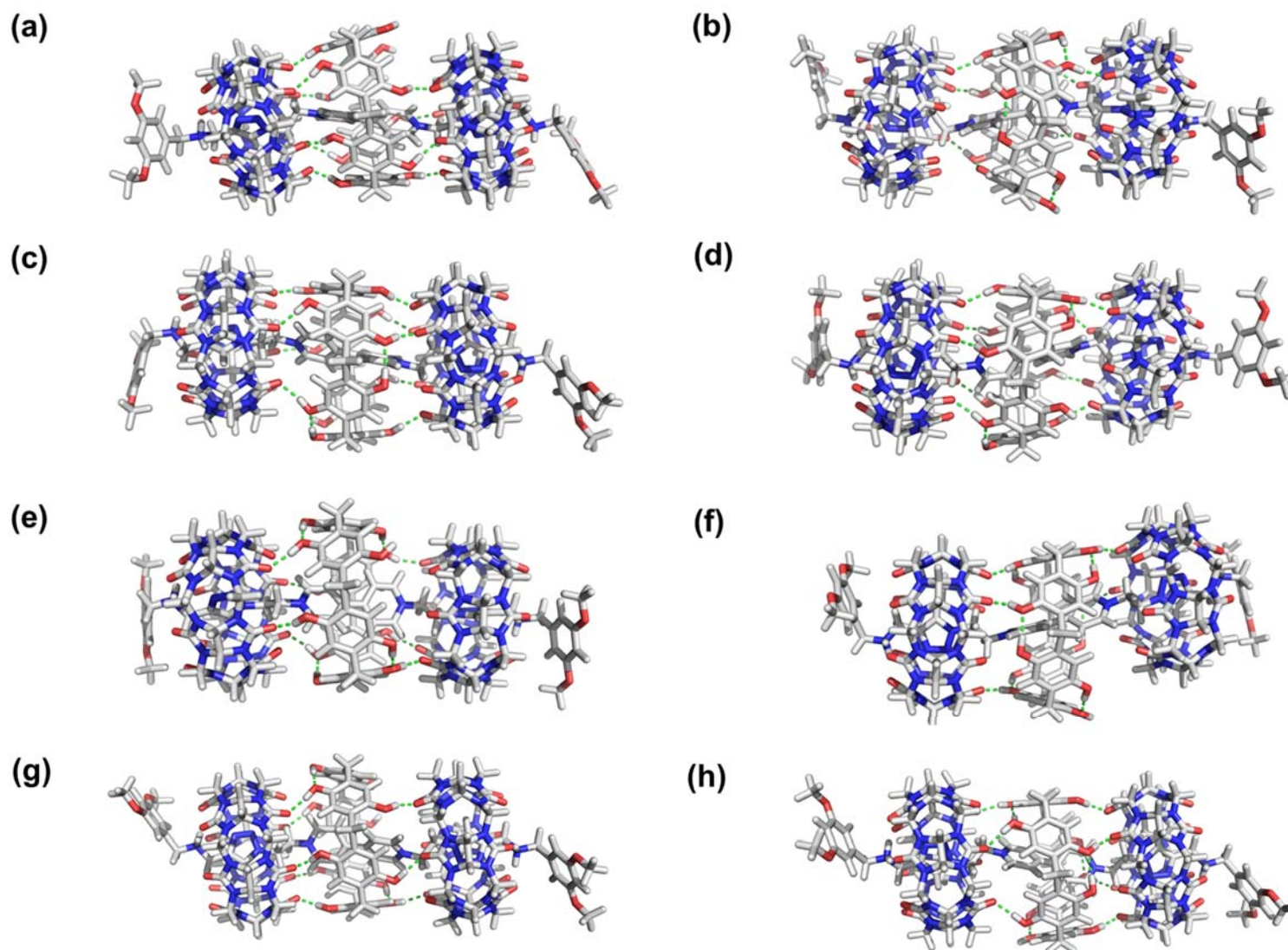


Figure S24. Lowest energy structures (a) – (h) of conformational isomers A – H of the hetero[4]rotaxane $2C4R_{P6} \cdot 4PF_6$ as a result of conformational search analysis.

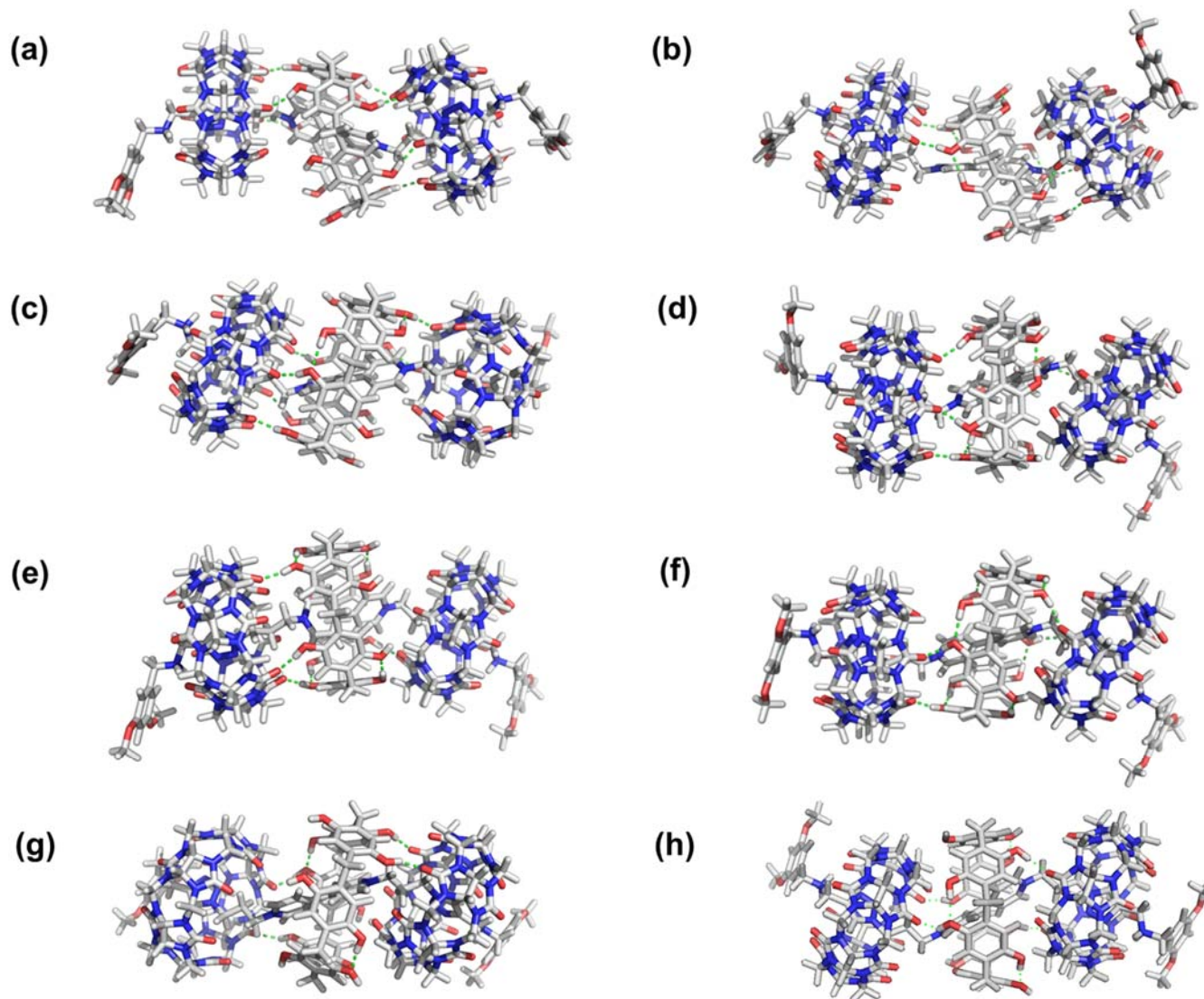


Figure S25. Lowest energy structures (a) – (h) of conformational isomers A – H of the hetero[4]rotaxane $3C4R_{P6} \cdot 4PF_6$ as a result of conformational search analysis⁶.

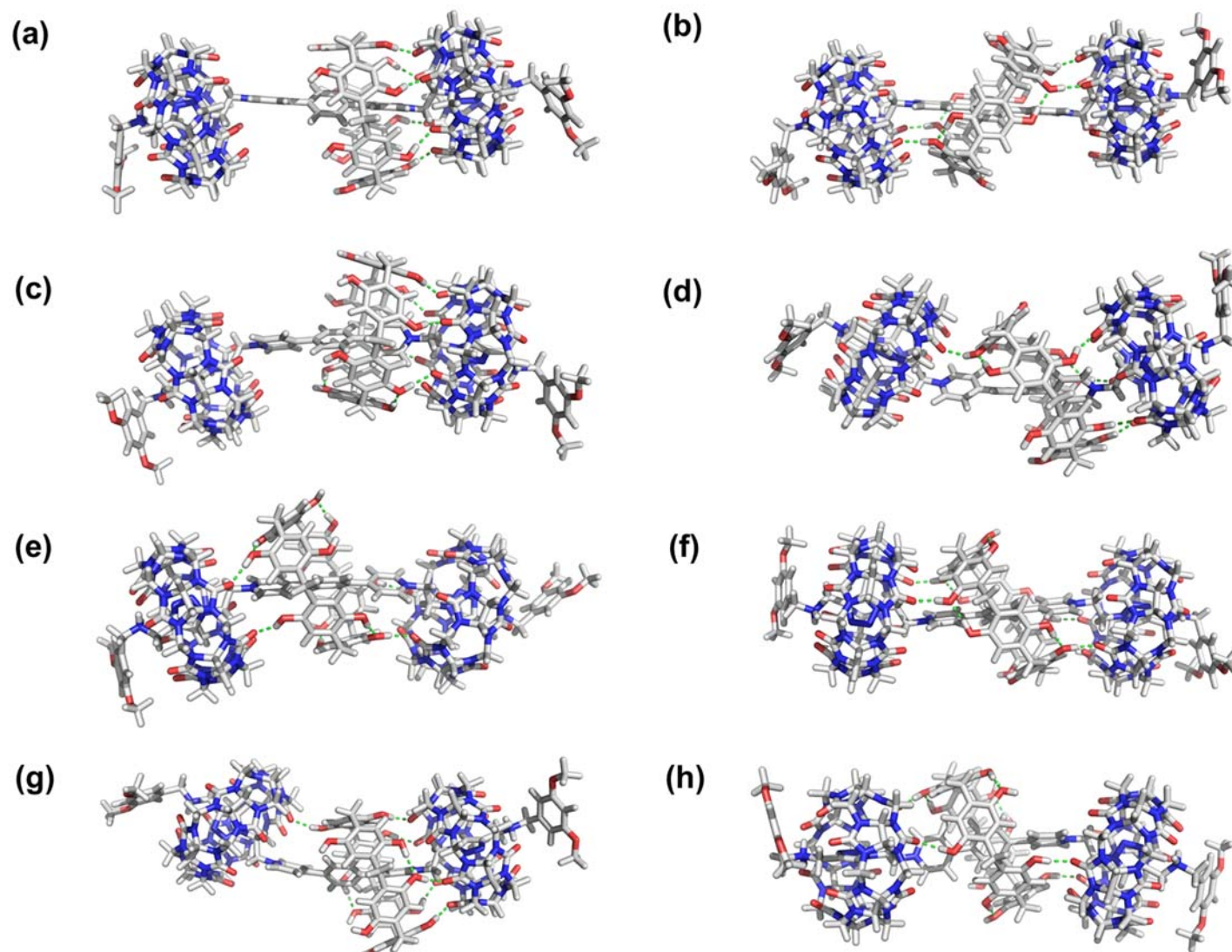


Figure S26. Lowest energy structures (a) – (h) of conformational isomers A – H of the hetero[4]rotaxane $2C4RexP_6 \cdot 4PF_6$ as a result of conformational search analysis⁷.

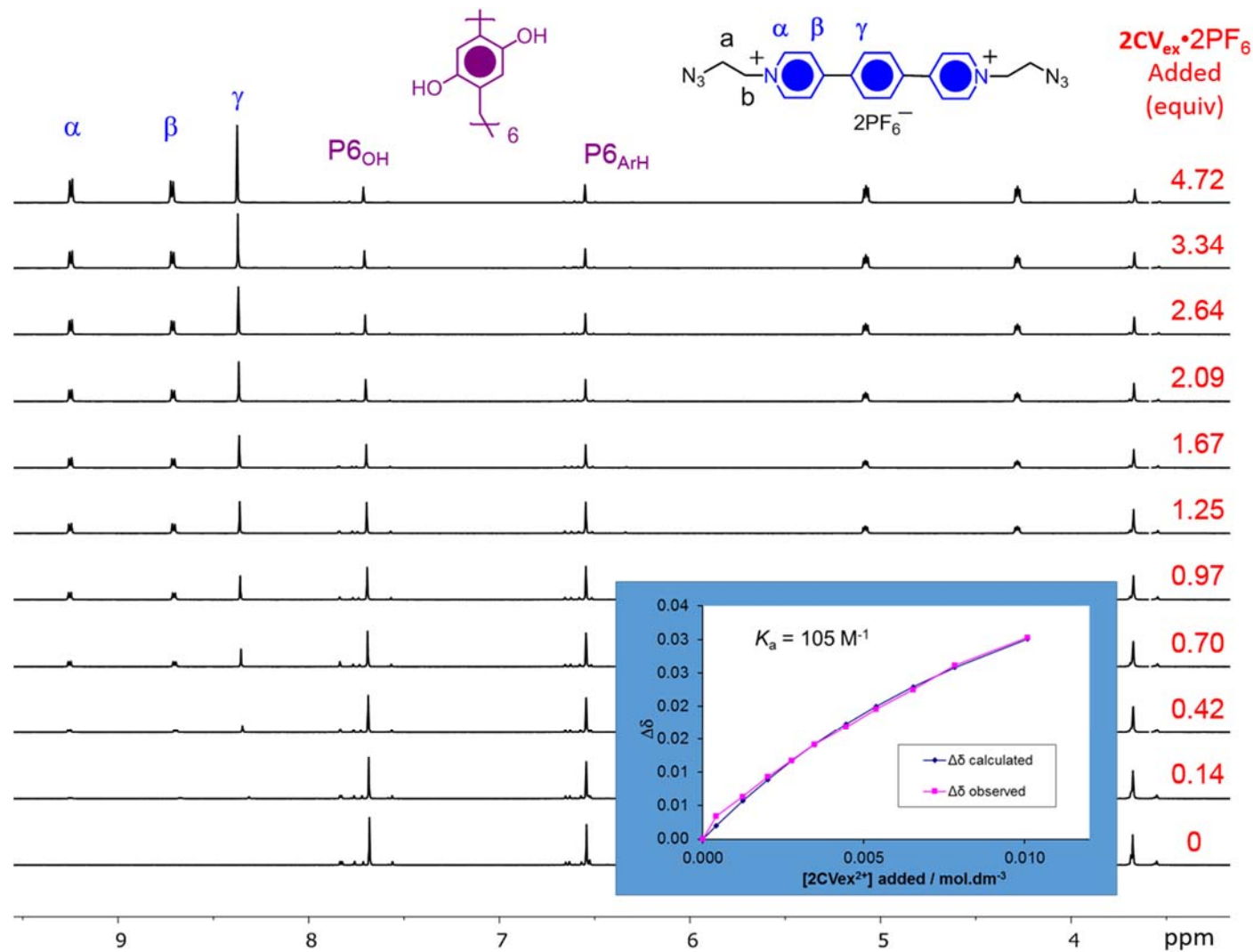


Figure S27. ^1H NMR spectra from the titration of P6 with $2\text{CV}_{\text{ex}}\cdot 2\text{PF}_6$ in $(\text{CD}_3)_2\text{CO}$ at 298 K. Experimental and calculated values for the NMR binding study of P6 (proton P6_{OH}) with $2\text{CV}_{\text{ex}}\cdot 2\text{PF}_6$ in $(\text{CD}_3)_2\text{CO}$, $K_a = 105 \text{ M}^{-1}$.

References

1. H. Li, Z. Zhu, A. C. Fahrenbach, B. M. Savoie, C. Ke, J. C. Barnes, J. Lei, Y. Zhao, L. M. Lilley, T. J. Marks, M. A. Ratner and J. F. Stoddart, *J Am Chem Soc*, 2013, **135**, 456-467.
2. Y. Ma, X. Chi, X. Yan, J. Liu, Y. Yao, W. Chen, F. Huang and J. Hou, *Org Lett*, 2012, **14**, 1532-1535.
3. C. Ke, N. L. Strutt, H. Li, X. Hou, K. J. Hartlieb, P. R. McGonigal, Z. Ma, J. Iehl, C. L. Stern, C. Cheng, Z. Zhu, N. A. Vermeulen, T. J. Meade, Y. Y. Botros and J. F. Stoddart, *J Am Chem Soc*, 2013, **135**, 17019-17030.
4. H. Nulwala, D. J. Burke, A. Khan, A. Serrano and C. J. Hawker, *Macromolecules*, 2010, **43**, 5474-5477.
5. J. C. Barnes, M. Juricek, N. L. Strutt, M. Frasconi, S. Sampath, M. A. Giesener, P. L. McGrier, C. J. Bruns, C. L. Stern, A. A. Sarjeant and J. F. Stoddart, *J Am Chem Soc*, 2013, **135**, 183-192.
6. One hydroquinone unit of conformational isomer A of **3C4R_{P6}•4PF₆** underwent oxygen-through-the-annulus rotation during the conformational search. As a result, the lowest energy structure of conformational isomer A of **3C4R_{P6}•4PF₆** shown is the lowest energy structure prior to the rotation of the hydroquinone unit.
7. Since the dumbbell of **2C4R_{exp6}•4PF₆** is long and rigid enough to accommodate the pillar[6]arene in the position either perpendicular or tilted at an angle to the dumbbell. A conformational search was performed on both positions and the lower energy structure was shown.